

NASA TECHNICAL
MEMORANDUM

NASA TM X-73369

USERS' GUIDE TO THE DATA OBTAINED BY THE
SKYLAB/ATM NASA-MARSHALL SPACE FLIGHT
CENTER/THE AEROSPACE CORPORATION S-056
X-RAY EXPERIMENT

(NASA-TM-X-73369) USER'S GUIDE TO THE DATA
OBTAINED BY THE SKYLAB/ATM NASA-MARSHALL
SPACE FLIGHT CENTER/THE AEROSPACE
CORPORATION S-056 X-RAY EXPERIMENT (NASA)
60 p HC A04/MF A01

N77-19977

Unclass

CSCI 03B G3/92

21606

December 1976

NASA



*George C. Marshall Space Flight Center
Marshall Space Flight Center, Alabama*

TECHNICAL REPORT STANDARD TITLE PAGE

1 REPORT NO. NASA TM X-73369	2. GOVERNMENT ACCESSION NO.	3 RECIPIENT'S CATALOG NO.
4 TITLE AND SUBTITLE Users' Guide to the Data Obtained by the Skylab/ATM NASA-Marshall Space Flight Center/The Aerospace Corporation S-056 X-Ray Experiment		5. REPORT DATE December 1976
7 AUTHOR(S)		6. PERFORMING ORGANIZATION CODE
9. PERFORMING ORGANIZATION NAME AND ADDRESS George C. Marshall Space Flight Center Marshall Space Flight Center, Alabama 35812		8. PERFORMING ORGANIZATION REPORT #
		10. WORK UNIT NO.
		11. CONTRACT OR GRANT NO.
12 SPONSORING AGENCY NAME AND ADDRESS National Aeronautics and Space Administration Washington, D. C. 20546		13. TYPE OF REPORT & PERIOD COVERED Technical Memorandum
		14. SPONSORING AGENCY CODE

15 SUPPLEMENTARY NOTES

Prepared by Space Sciences Laboratory, Science and Engineering

16. ABSTRACT

The ATM/S-056 X-Ray Experiment operated successfully on Skylab from May 1973 to February 1974. The S-056 observations consist of 27 000 photographs (filterheliograms) obtained by the X-ray telescope and 1100 h of proportional counter data obtained by the X-ray event analyzer in the soft X-ray region of the solar spectrum. This report contains a description of the S-056 data together with additional relevant information that may be needed by users of the data. Although the report is intended primarily to describe the data that were sent to the National Space Science Data Center, it should also be useful to other users.

17. KEY WORDS

18. DISTRIBUTION STATEMENT

Unclassified — Unlimited

E. Tandberg-Hanssen

19 SECURITY CLASSIF. (of this report)

20 SECURITY CLASSIF. (of this page)

21 NO. OF PAGES

22 PRICE

Unclassified

Unclassified

58

NTIS

ACKNOWLEDGMENTS

Contributions to this guide in the form of information, comments, figures, and text were made by a number of individuals. In addition to certain members of the S-056 Mission Scientific Team, the following persons, who are members of the S-056 data analysis groups at MSFC and Aerospace, should be mentioned: R. M. Broussard and J. A. Vorpahl of The Aerospace Corporation, E. J. Reichmann of MSFC, and D. M. Speich and J. B. Smith of NOAA (located at MSFC).

W. Henze was supported by NASA Contracts NAS8-26442 and NAS8-31908.

**USERS' GUIDE TO THE DATA OBTAINED BY THE SKYLAB/ATM
NASA MARSHALL SPACE FLIGHT CENTER/THE AEROSPACE
CORPORATION S-056 X-RAY EXPERIMENT**

Editor:

William Henze, Jr.
Teledyne Brown Engineering

Principal Investigators, S-056 Data Analysis:

E. Tandberg-Hanssen, Marshall Space Flight Center
J. H. Underwood, Stanford University

Mission Scientific Team:

MSFC: J. E. Milligan, Principal Investigator
A. C. deLoach
R. B. Hoover
J. P. McGuire
R. M. Wilson
H. B. Hester
J. W. Berry

AEROSPACE: J. H. Underwood
G. A. Chapman
E. N. Frazier
T. J. Janssens
D. L. McKenzie
V. A. Stevens

TABLE OF CONTENTS

	Page
I. INTRODUCTION	1
A. Scope	1
B. Materials Submitted to NSSDC	2
II. X-RAY TELESCOPE	3
A. Instrument	3
1. Description	3
2. Point Spread Function	5
3. Vignetting	7
4. Filter Transmission and Mirror Reflectivity	7
B. Operating Modes	9
C. Films and Calibration	16
1. Film Description — Originals and Copies	16
2. Format of Film Sensitometry	18
3. Calibration Data	18
D. Solar Observations and Ancillary Data	26
1. Frame Listings	26
2. Image Position and Orientation	26
3. Data Block Lights	28
4. Specialized Catalogs	30
E. Telescope Housekeeping Data (Microfilm Records)	30
F. Quantitative Analysis of Filterheliograms	39
III. X-RAY EVENT ANALYZER	42
A. Instrument Description	42
B. Proportional Counter Response	44
C. X-REA Observations	44
1. Microfilm Records	44
2. Specialized Catalog	50
D. Quantitative Analysis of X-REA Observations	51
REFERENCES	52

PRECEDING PAGE BLANK NOT FILMED

LIST OF ILLUSTRATIONS

Figure	Title	Page
1.	Cutaway diagram of S-056 experiment	4
2.	Schematic diagram of S-056 X-ray telescope optics	4
3.	S-056 point spread function	6
4.	Geometrical vignetting	8
5.	Product of filter transmission and telescope efficiency in the 0 to 24 Å region (Filters 1 and 2)	11
6.	Product of filter transmission and telescope efficiency in the 0 to 24 Å region (Filters 3, 4, and 5)	12
7.	Product of filter transmission and telescope efficiency in the 26 to 50 Å region (Filter 3)	13
8.	Appearance of typical sensitometry sets.....	24
9.	Format of S-056 frame	27
10.	Data block configuration	29
11.	Example of printout of S-056 temperature data on microfilm	38
12.	Example of printout of S-056 discrete event and current data on microfilm.....	40
13.	Example of discrete event data associated with a Super-Long exposure (Filter 1)	41
14.	Aluminum counter response	47
15.	Beryllium counter response	48
16.	Example of printouts of S-056 X-REA data on microfilm	49

LIST OF TABLES

Table	Title	Page
1.	S-056 X-Ray Telescope Geometrical Properties	5
2.	S-056 Point Spread Function.....	7
3.	Geometrical Vignetting	9
4.	Filter Characteristics of S-056 X-Ray Telescope.....	10
5.	S-056 Combined Filter-Telescope Transmission	14
6.	Exposure Times for S-056 X-Ray Photographs	15
7.	S-056 Film Usage.....	17
8.	Load 1, Identification of Sensitometry Sets	19
9.	Load 2, Identification of Sensitometry Sets	20
10.	Load 3, Identification of Sensitometry Sets	21
11.	Load 4, Identification of Sensitometry Sets	22
12.	Load 5, Identification of Sensitometry Sets	23
13.	S-056 Film Calibration	25
14.	Correlation Between Date and Various "Days," Microfilm Availability for 6 h Periods, Mission Milestones	31
15.	Temperature and Current Measurements	36
16.	Discrete Event Measurements	37
17.	X-Ray Event Analyzer Properties	43
18.	Aluminum Counter Response	45
19.	Beryllium Counter Response	46

USERS' GUIDE TO THE DATA OBTAINED BY THE SKYLAB/ATM
NASA-MARSHALL SPACE FLIGHT CENTER/THE AEROSPACE
CORPORATION S-056 X-RAY EXPERIMENT

I. INTRODUCTION

A. Scope

The purpose of this guide is to aid users of the data obtained by the Skylab/Apollo Telescope Mount (ATM) NASA-Marshall Space Flight Center/The Aerospace Corporation S-056 X-Ray Experiment. It contains a description of the observations and how they were obtained. Although the preparation of this report was intended primarily to satisfy the requirements of the National Space Science Data Center (NSSDC), the experimenters hope that it will also be useful to others, such as members of or visitors to the experimenters' institutions and those who obtain access to the data through sources other than the NSSDC.

The overall objective of the S-056 experiment was to study the structure and evolution of the solar corona at X-ray wavelengths. To accomplish this goal, the experiment package contained two instruments for observing the Sun in the soft X-ray spectral region. The primary instrument was an X-ray telescope used for direct photography on 35 mm film of a field of view normally containing the entire solar disk. The use of five broad-band X-ray filters provided some spectral information. The selection of filters, exposure times, and intervals between exposures was incorporated in preset sequences that could be chosen by the Skylab crew member to optimize the observations of a particular solar phenomenon. A second scientific instrument was the X-ray event analyzer (X-REA), containing two proportional counters with pulse-height analyzers to monitor the flux from the entire Sun and obtain coarse spectral information.

The S-056 experiment operated successfully throughout the manned portions of the Skylab mission from May 1973 to February 1974. A detailed description of the operational performance of the experiment is given in "The Skylab ATM/S-056 Solar X-Ray Telescope: Design and Performance," a NASA Technical Note scheduled for publication in 1977. Also, the S-056 experiment is included in an overall evaluation of the ATM performance during the Skylab mission [1].

Sections II and III of this guide describe the use of data from the X-ray telescope and X-REA, respectively. They include brief descriptions of the instruments with all necessary instrumental parameters, the modes of operation, calibration data, and descriptions of the form of the observations. Also included are outlines on the quantitative use of the observations.

B. Materials Submitted to NSSDC

Materials already sent or to be sent to NSSDC for use in conjunction with this guide include the following:

1. Film copies — One set of positive copies exposed for bright features and one set exposed for faint features of the four loads of black-and-white film (total of 8 rolls of film). Two sets of positive black-and-white copies exposed for bright features and two sets exposed for faint features of the load of color film (total of 4 rolls of film).

2. Microfilm — One copy of 565 rolls of microfilm (each covering a 6-h period) containing X-REA counts, housekeeping data, and temperature data for various locations in the experiment package.

3. Publications —

"S-056 Frame Listing" (in loose-leaf, three-ring binder).

"Atlas of Skylab ATM/S056 Super-Long Exposures and Stepped-Image Frames" [2].

"The Skylab ATM/S-056 Solar X-Ray Telescope: Design and Performance" (in preparation).

"The Skylab ATM/S-056 X-Ray Event Analyzer: Instrument Description, Parameter Determination, and Analysis Example (15 June 1973 1B/M3 Flare)" [3].

"Film Calibration for the Skylab ATM/S-056 X-Ray Telescope" (in preparation).

"Compilation of Flares and Transients Observed by the S-056 Solar X-Ray Telescope During the Skylab Missions" [4].

"Atlas of Skylab ATM/S056 Coronal Hole Observations" [5].

"Skylab ATM/S-056 X-Ray Event Analyzer Observations Versus Solar Flare Activity: An Event Compilation" (in preparation).

II. X-RAY TELESCOPE

A. Instrument

This section contains a brief description of the S-056 X-ray telescope and provides information concerning instrumental properties needed to interpret the observations. These instrumental properties include the telescope collecting area, focal length, point-spread function, vignetting, filter transmissions, and mirror reflectivity.

1. Description. A cutaway drawing of the S-056 experiment package is shown in Figure 1. The glancing-incidence X-ray telescope was of Wolter's Type 1 configuration comprised of two mirrors, a paraboloid and hyperboloid, made of fused silica. Figure 2 shows a schematic diagram of the telescope optics. A shield and first stop prevented solar radiation from heating the front of the instrument and also shielded the film from direct X-rays. The entrance aperture was thus an annulus. A second stop within the telescope prevented rays that had undergone only a single reflection from reaching the film.

The camera assembly consisted of a filter wheel containing five X-ray filters and one visible light filter, a shutter to control exposure time, a replaceable film magazine holding 305 m of film, an airlock door to maintain humidity inside the magazine, and an optical system to project the image of an array of data block lights onto the film. The data block lights, to be described later, provided auxiliary information about each exposure.

The whole instrument was mounted rigidly to the ATM spar by four thermal isolation mounts and thus shared the pointing of the entire spar. There were no provisions for internal motions of the S-056 telescope relative to the ATM spar.

The important geometrical properties of the telescope are given in Table 1. More detailed descriptions of the S-056 instrument have been or will be published by Walsh et al. [6] and Underwood et al. [7] and in "The Skylab ATM/S-056 Solar X-Ray Telescope: Design and Performance," which is scheduled for publication in 1977.

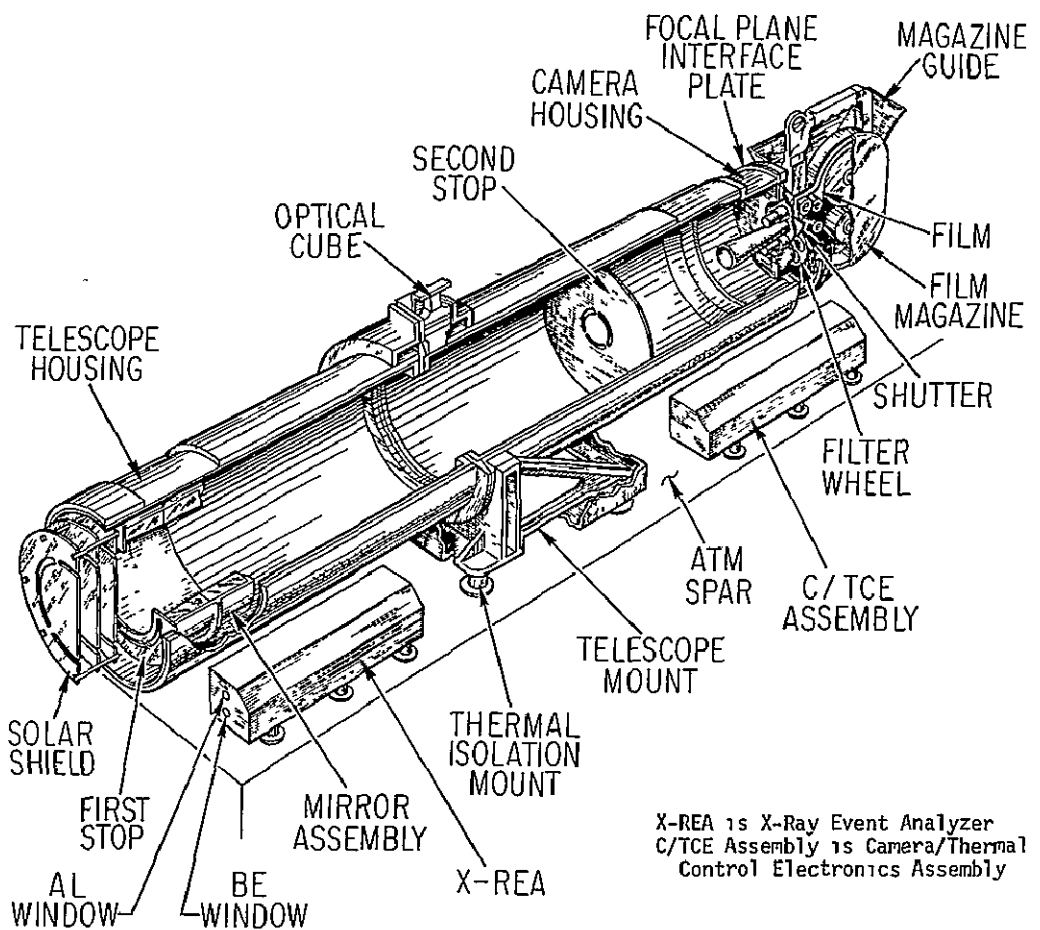


Figure 1. Cutaway diagram of S-056 experiment.

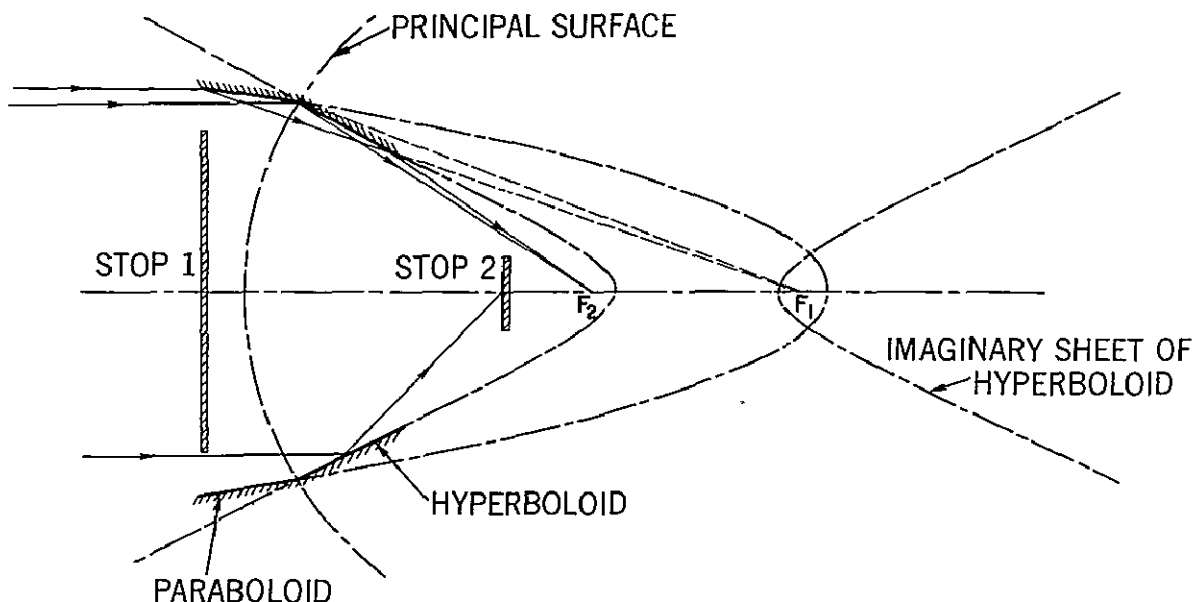


Figure 2. Schematic diagram of S-056 X-ray telescope optics
(the film plane is at F₂).

TABLE 1. S-056 X-RAY TELESCOPE GEOMETRICAL PROPERTIES

Focal Length	190.3 cm
Collecting Area	14.66 cm ²
Usable Field of View	38 arc min
Plate Scale	9.23 μ m/arc s
Internal Diameter at Intersection of Two Mirrors	24.35 cm
Average Glancing Angle of Incidence on Each Mirror for Rays Parallel to the Optical Axis	0.916 degree

2. Point Spread Function. The point spread function is the intensity distribution in the image of a point source. The on-axis S-056 point spread function is shown in Figure 3 and is tabulated in Table 2. It has a sharp core with full width at half maximum of approximately 2 arc s and broad wings caused by zonal aberrations and scattering from the surfaces of the mirrors. The sharpness of the core means that the telescope has high resolving power, and that for many applications it is not necessary to try to improve the resolution by deconvolution. However, the existence of broad wings means that considerable energy is removed from the central core; for applications in which accurate intensity measurements are needed, it may be desirable to use deconvolution to correct the intensity distribution on observed images. This is most likely to be important for narrow features and for faint features near bright regions.

The point spread function given in the figure and table is valid for portions of images near the optical axis; however, it can usually be used out to angles of 16 arc min off axis (i.e., the entire solar disk when pointed at the center of the Sun) without introducing large errors. Away from the optical axis, the point spread function deviates from rotational symmetry; the sharp core is no longer centered in the halo of the wings. At very large angles, greater than approximately 19 arc min, the point spread function becomes elongated and exhibits lobes caused by the supports for the central portion of the stops and the solar shield.

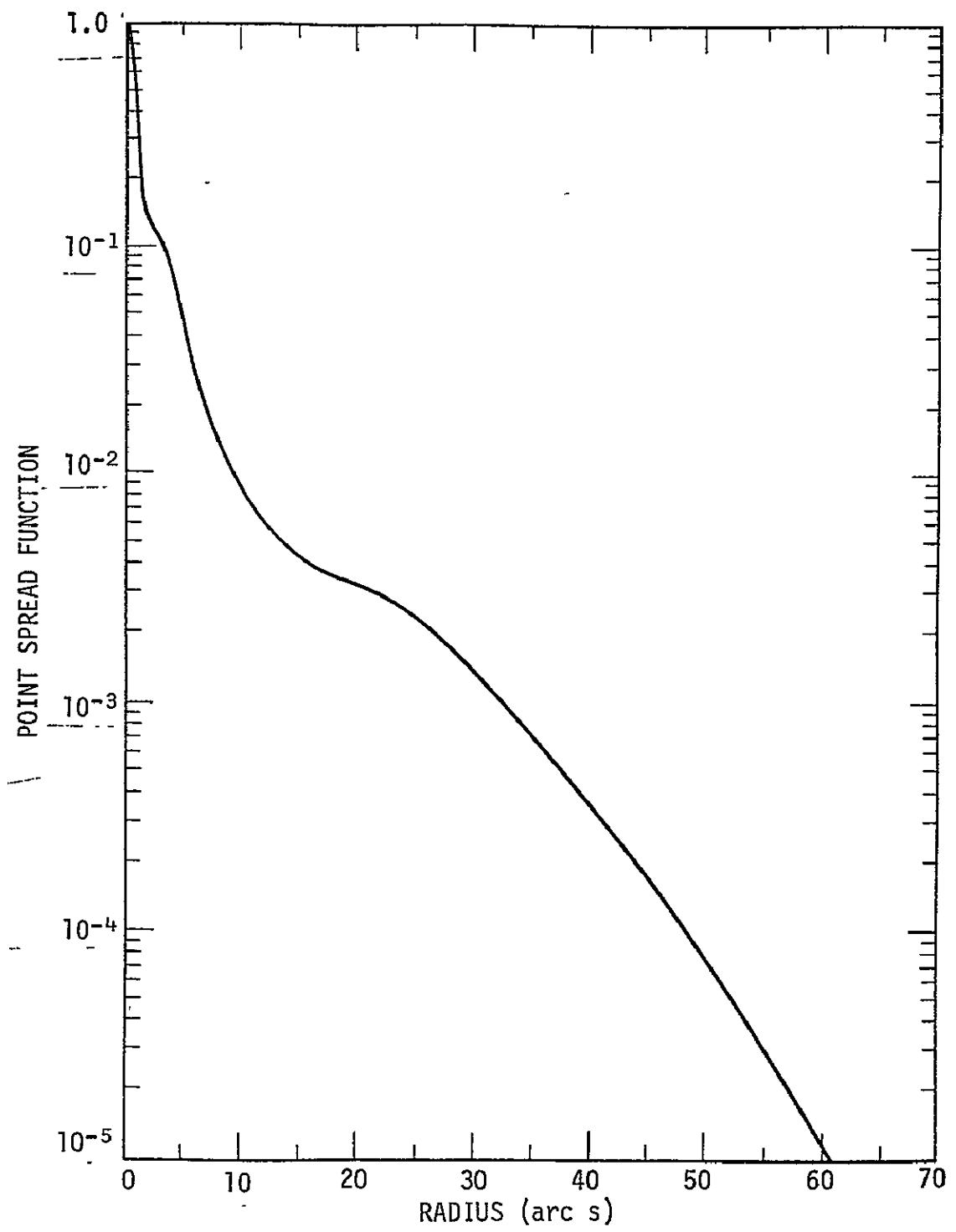


Figure 3. S-056 point spread function.

TABLE 2. S-056 POINT SPREAD FUNCTION

RADIUS (arc s)	POINT SPREAD FUNCTION	RADIUS (arc s)	POINT SPREAD FUNCTION
0.0	1.0	4.0	8.6(-2)
0.1	9.8(-1)	5.0	4.8(-2)
0.2	9.5(-1)	7.0	1.8(-2)
0.3	8.8(-1)	10.0	8.8(-3)
0.5	7.4(-1)	15.0	4.3(-3)
0.8	5.2(-1)	20.0	3.2(-3)
1.0	4.2(-1)	25.0	2.4(-3)
1.2	3.1(-1)	30.0	1.4(-3)
1.5	1.30(-1)	40.0	3.6(-4)
2.0	1.25(-1)	50.0	8.0(-5)
3.0	1.08(-1)	60.0	1.2(-5)

3. Vignetting. Vignetting is defined as the variation with angle off-axis of the telescope transmission. It can also be thought of as the flux distribution in the image plane due to a uniformly bright source over the whole sky visible to the telescope. This section is concerned only with the geometrical vignetting, i.e., the effects of the stops and the size of the mirrors on off-axis rays. Although variations in mirror reflectivity as a function of both angle of incidence and wavelength also contribute to the overall vignetting, these effects will be ignored to a first approximation.

The geometrical vignetting as a function of angle off-axis is shown in Figure 4 and tabulated in Table 3. (These values were calculated using a ray-trace analysis by J. William Foreman, Jr., and Joseph M. Cardone of Montevallo Research Associates.) As can be seen from the figure, the vignetting function decreases almost linearly from unity on axis to approximately 77 percent at an angle of 19 arc min off axis. At larger angles, the vignetting function decreases more rapidly. Thus, when the ATM was pointed near one limb and the solar feature being analyzed was near the opposite limb, vignetting had significant effect.

4. Filter Transmission and Mirror Reflectivity. The S-056 X-ray telescope contained five thin filters of metallic foil to isolate broad wavelength bands in the soft X-ray spectrum. A sixth filter yielded a visible light image in the red region of the spectrum. The filters were mounted on a wheel whose position was normally changed after each exposure.

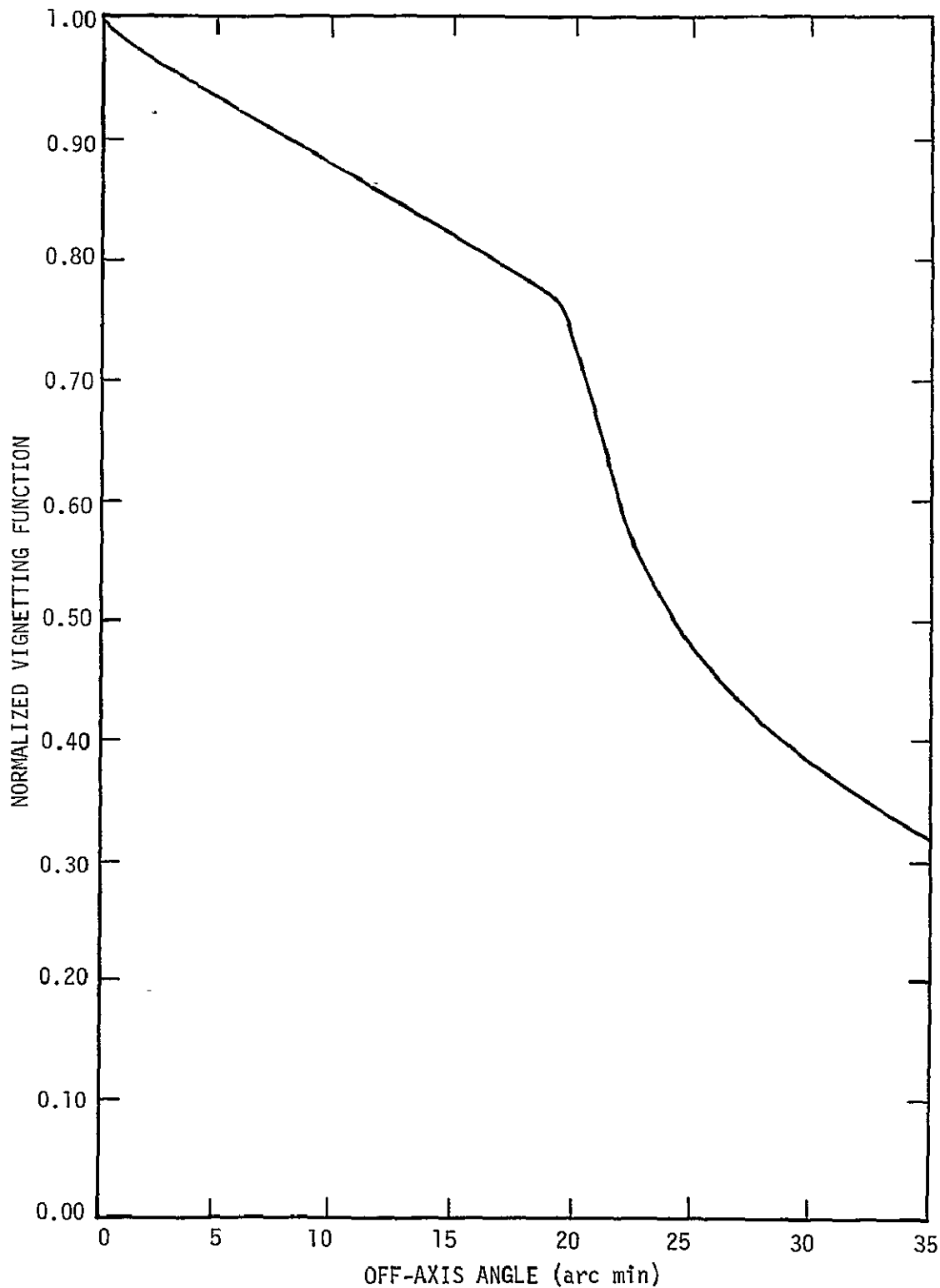


Figure 4. Geometrical vignetting.

TABLE 3. GEOMETRICAL VIGNETTING

OFF-AXIS ANGLE (arc min)	VIGNETTING FUNCTION	OFF-AXIS ANGLE (arc min)	VIGNETTING FUNCTION	OFF-AXIS ANGLE (arc min)	VIGNETTING FUNCTION
0	1.0000	12	0.8521	24	0.5093
1	0.9806	13	0.8400	25	0.4805
2	0.9681	14	0.8287	26	0.4555
3	0.9575	15	0.8178	27	0.4337
4	0.9456	16	0.8054	28	0.4137
5	0.9331	17	0.7943	29	0.3962
6	0.9222	18	0.7831	30	0.3811
7	0.9109	19	0.7711	31	0.3656
8	0.8983	20	0.7346	32	0.3514
9	0.8870	21	0.6613	33	0.3390
10	0.8750	22	0.5889	34	0.3282
11	0.8635	23	0.5444	35	0.3194

The characteristics of the filters are summarized in Table 4. The product of the filter transmission and the reflectivities of the mirrors at the average angle of incidence is shown in Figures 5 through 7 and tabulated in Table 5 as a function of wavelength for each of the X-ray filters.

During the second manned mission (SL3), Filter 3 developed a light leak that allowed visible light to expose part of the frame. Although X-ray data were still recorded with this filter on portions of the frame not affected by the leak, the images are usually not very useful. The condition of Filter 3 became progressively worse during the remainder of the Skylab mission.

B. Operating Modes

The S-056 telescope was capable of operating only during those portions of the three manned missions when the ATM console was attended by a Skylab astronaut. Several operating modes were available in which filter changes and selection of exposure time and time between exposures were normally done in

TABLE 4. FILTER CHARACTERISTICS OF S-056 X-RAY TELESCOPE

FILTER	MATERIAL	THICKNESS (mg cm ⁻²)	WAVELENGTH RANGE (Å)	WAVELENGTH AT PEAK TRANSMISSION (Å)	PEAK TRANSMISSION
1	0.50-mil (12.7 µm) Aluminum	3.42	8 to 14	8.0	0.17
2	0.25-mil (6.35 µm) Aluminum	1.71	8 to 18	8.0	0.33
3	0.086-mil (2.2 µm) Titanium	0.99	6 to 13 27 to 40	7.5	0.093
4	1-mil (25.4 µm) Beryllium	4.62	6 to 16	7.9	0.29
5	3-mil (76.2 µm) Beryllium	13.86	6 to 12	7.4	0.097
6	Multilayer Dielectric Interference Filter		80 (FWHM)	6328	

Note: The wavelength range is the region where the transmission exceeds 1 percent of the peak transmission for that filter. The transmission used for both the peak and the range is the product of the filter transmission and the reflectivities of the mirrors.

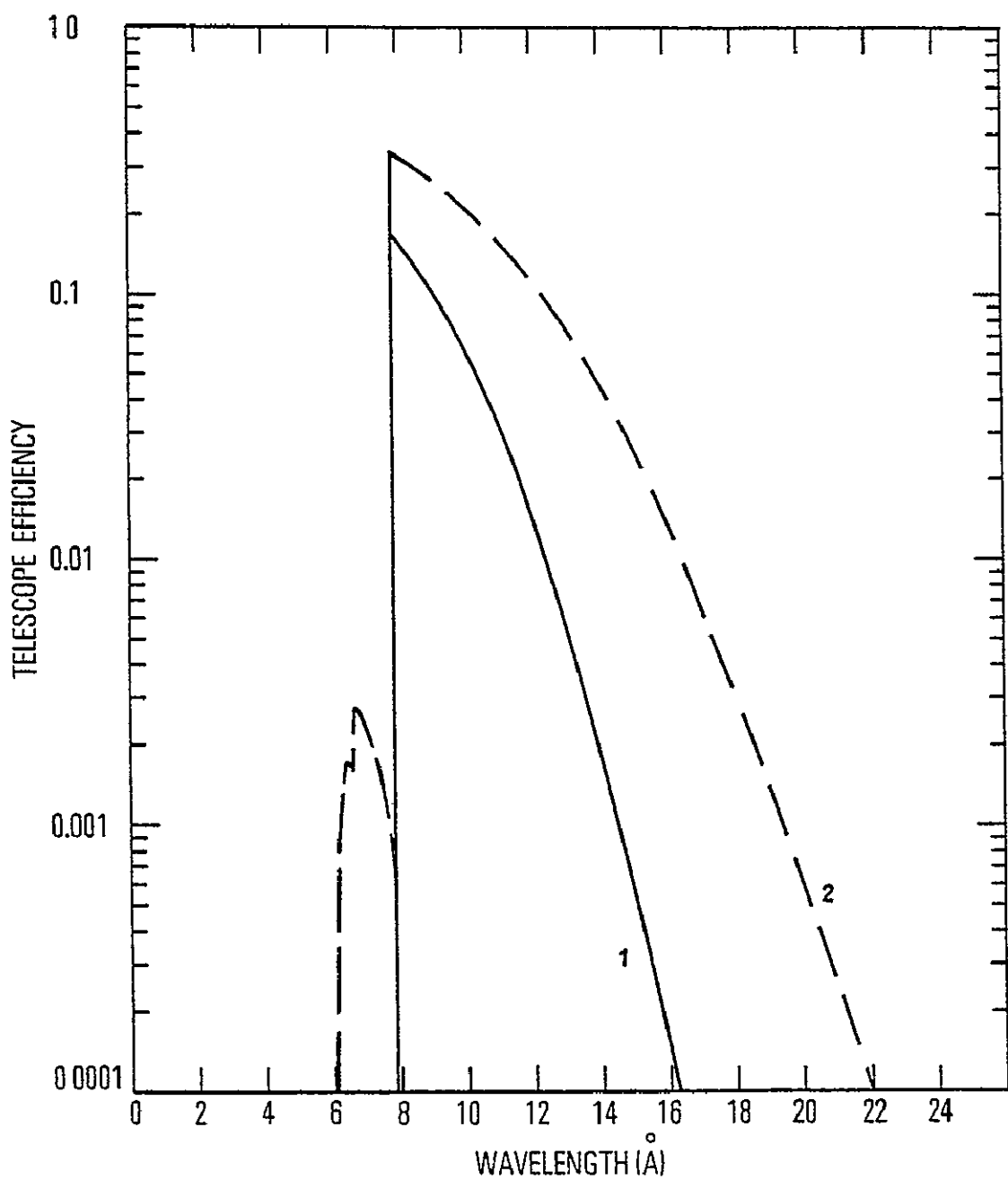


Figure 5. Product of filter transmission and telescope efficiency in the 0 to 24 \AA region (Filters 1 and 2).

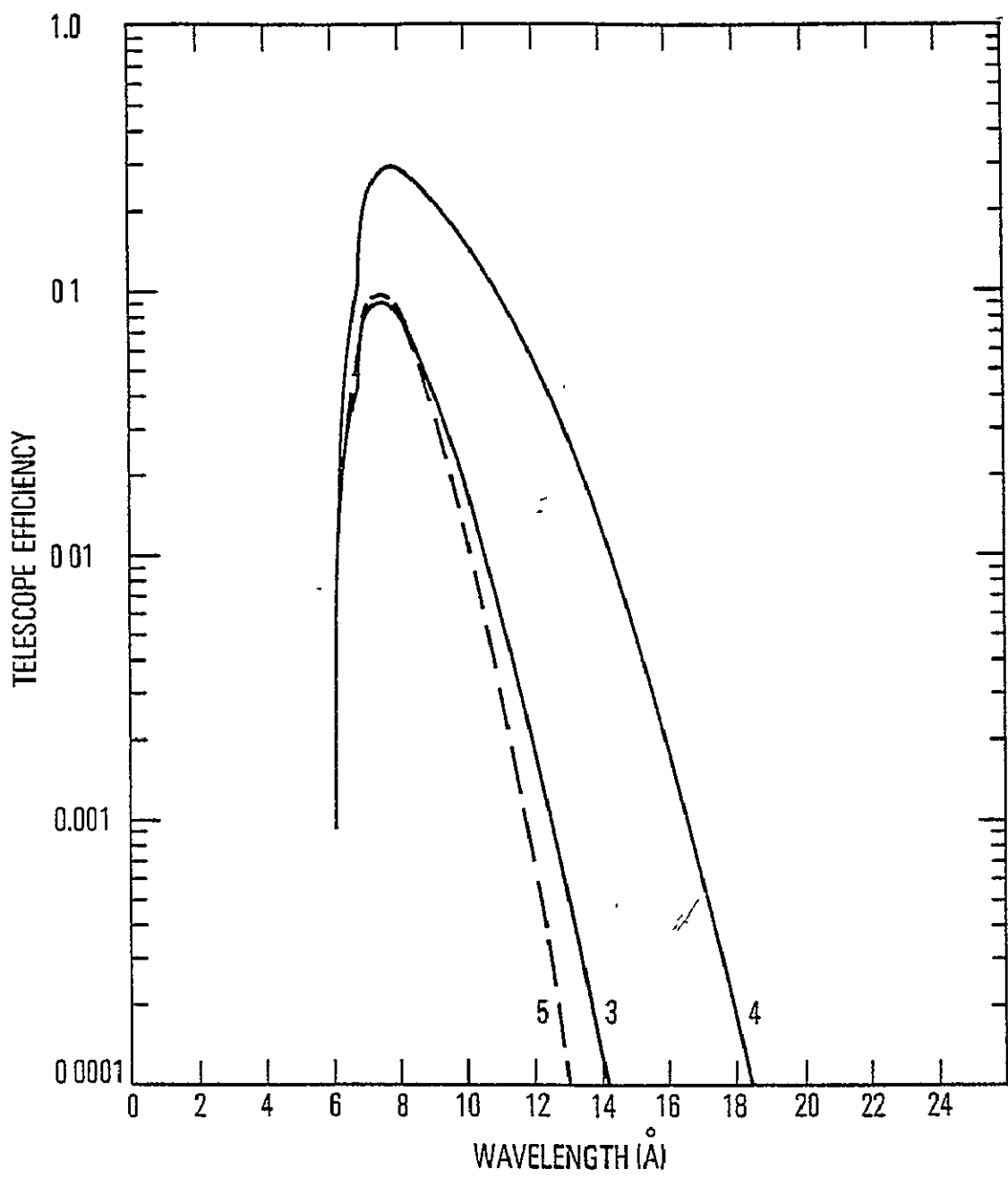


Figure 6. Product of filter transmission and telescope efficiency in the 0 to 24 Å region (Filters 3, 4, and 5).

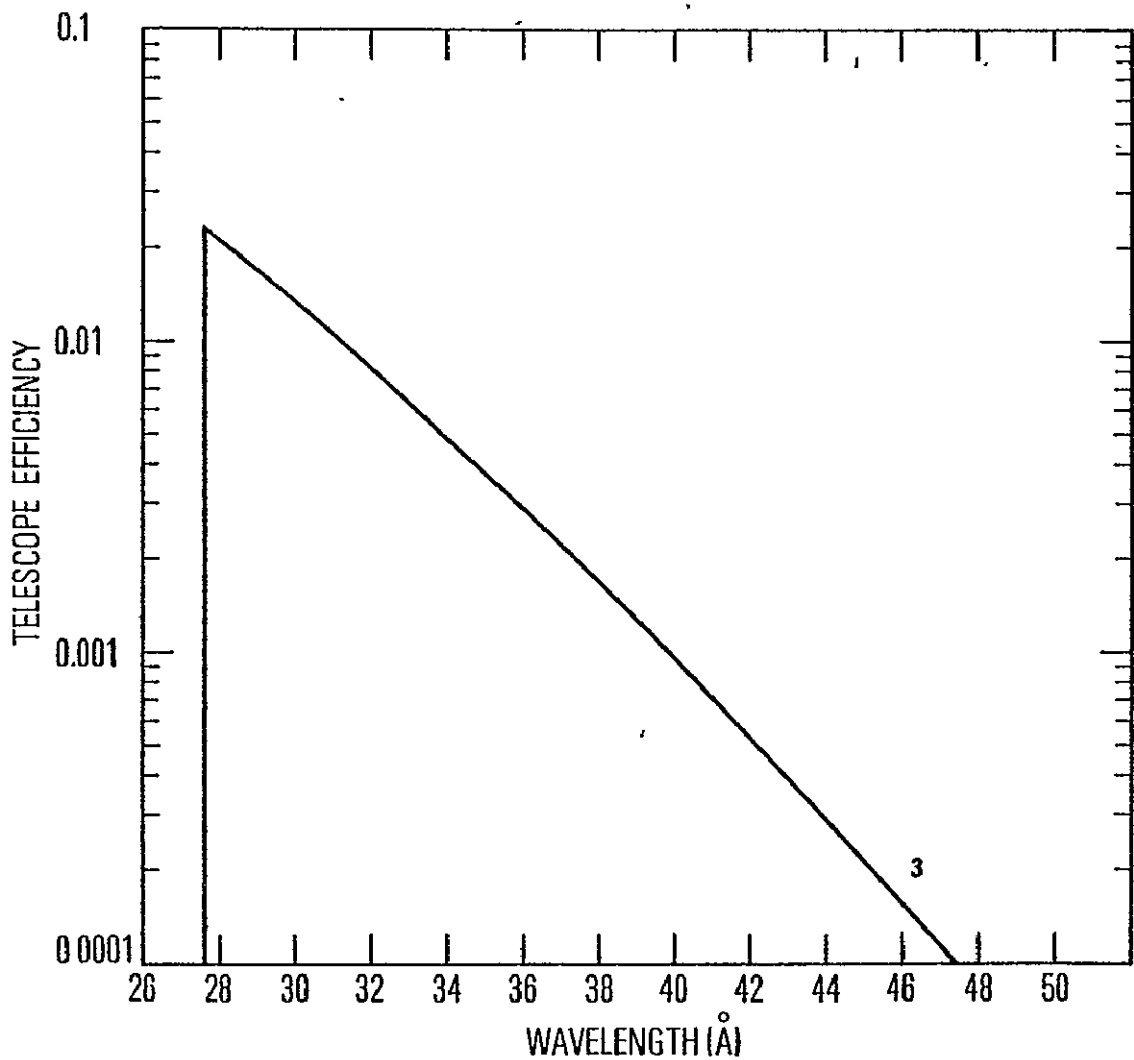


Figure 7. Product of filter transmission and telescope efficiency in the 26 to 50 Å region (Filter 3).

preset sequences chosen by the astronaut to optimize the observations of a particular solar phenomenon. Each sequence had to be initiated by the astronaut. Within each mode, three sets of exposure times were available: Short, Normal, and Long. The Short exposures were intended to be a factor of 3.2 shorter than the Normal, and the Long exposures a factor of 3.2 longer than the Normal. The average exposure times for the Patrol and Active modes are given in Table 6. The values for the Active and Patrol Short modes were determined statistically; they should be used in place of the values indicated by the data lights (to be described later) which can be read only to the nearest one-fourth second. The Patrol Long and Normal exposure times can be determined with sufficient accuracy from the data lights.

TABLE 5. S-056 COMBINED FILTER-TELESCOPE TRANSMISSION

WAVELENGTH Å	FILTER					WAVELENGTH Å	FILTER 3
	1	2	3	4	5		
6.1	3.69(-6)	2.04(-4)	2.37(-3)	4.61(-3)	2.62(-3)	27.3	2.35(-2)
6.2	1.22(-5)	8.04(-4)	1.04(-2)	2.08(-2)	1.15(-2)	27.5	2.25(-2)
6.3	1.74(-5)	1.38(-3)	2.00(-2)	4.12(-2)	2.21(-2)	28.0	2.02(-2)
6.4	1.80(-5)	1.72(-3)	2.81(-2)	5.95(-2)	3.09(-2)	28.5	1.81(-2)
6.5	1.54(-5)	1.79(-3)	3.29(-2)	7.16(-2)	3.61(-2)	29.0	1.62(-2)
6.6	1.14(-5)	1.62(-3)	3.37(-2)	7.54(-2)	3.68(-2)	29.5	1.45(-2)
6.7	1.56(-5)	2.73(-3)	6.43(-2)	1.48(-1)	7.00(-2)	30.0	1.29(-2)
6.8	1.23(-5)	2.65(-3)	7.12(-2)	1.69(-1)	7.72(-2)	30.5	1.15(-2)
6.9	9.45(-6)	2.52(-3)	7.72(-2)	1.89(-1)	8.33(-2)	31.0	1.02(-2)
7.0	7.06(-6)	2.34(-3)	8.23(-2)	2.08(-1)	8.84(-2)	31.5	9.09(-3)
7.1	5.14(-6)	2.14(-3)	8.63(-2)	2.26(-1)	9.22(-2)	32.0	8.06(-3)
7.2	3.67(-6)	1.92(-3)	8.94(-2)	2.41(-1)	9.49(-2)	32.5	7.14(-3)
7.3	2.56(-6)	1.69(-3)	9.14(-2)	2.55(-1)	9.64(-2)	33.0	6.31(-3)
7.4	1.75(-6)	1.48(-3)	9.25(-2)	2.67(-1)	9.68(-2)	33.5	5.57(-3)
7.5	1.17(-6)	1.27(-3)	9.26(-2)	2.77(-1)	9.62(-2)	34.0	4.92(-3)
7.6	7.73(-7)	1.07(-3)	9.18(-2)	2.84(-1)	9.46(-2)	34.5	4.33(-3)
7.7	5.00(-7)	8.99(-4)	9.02(-2)	2.89(-1)	9.22(-2)	35.0	3.81(-3)
7.8	3.17(-7)	7.43(-4)	8.79(-2)	2.92(-1)	8.90(-2)	35.5	3.34(-3)
7.9	1.98(-7)	6.07(-4)	8.50(-2)	2.93(-1)	8.51(-2)	36.0	2.93(-3)
8.0	1.68(-1)	3.33(-1)	8.15(-2)	2.92(-1)	8.07(-2)	36.5	2.57(-3)
8.1	1.63(-1)	3.31(-1)	7.75(-2)	2.88(-1)	7.60(-2)	37.0	2.24(-3)
8.2	1.58(-1)	3.28(-1)	7.32(-2)	2.83(-1)	7.09(-2)	37.5	1.96(-3)
8.3	1.51(-1)	3.22(-1)	6.86(-2)	2.76(-1)	6.56(-2)	38.0	1.71(-3)
8.4	1.44(-1)	3.14(-1)	6.38(-2)	2.67(-1)	6.02(-2)	38.5	1.49(-3)
8.5	1.38(-1)	3.09(-1)	5.97(-2)	2.60(-1)	5.56(-2)	39.0	1.29(-3)
8.6	1.31(-1)	3.02(-1)	5.55(-2)	2.52(-1)	5.09(-2)	39.5	1.12(-3)
8.7	1.25(-1)	2.95(-1)	5.15(-2)	2.44(-1)	4.66(-2)	40.0	9.74(-4)
8.8	1.19(-1)	2.88(-1)	4.78(-2)	2.36(-1)	4.25(-2)	40.5	8.43(-4)
8.9	1.13(-1)	2.82(-1)	4.43(-2)	2.29(-1)	3.88(-2)	41.0	7.29(-4)
9.0	1.07(-1)	2.75(-1)	4.10(-2)	2.21(-1)	3.52(-2)	41.5	6.30(-4)
9.5	8.12(-2)	2.42(-1)	2.72(-2)	1.84(-1)	2.12(-2)	42.0	5.43(-4)
10.0	6.01(-2)	2.10(-1)	1.74(-2)	1.50(-1)	1.20(-2)	42.5	4.68(-4)
10.5	4.32(-2)	1.81(-1)	1.07(-2)	1.20(-1)	6.41(-3)	43.0	4.02(-4)
11.0	3.03(-2)	1.54(-1)	6.37(-3)	9.41(-2)	3.22(-3)	43.5	3.46(-4)
11.5	2.06(-2)	1.29(-1)	3.64(-3)	7.19(-2)	1.51(-3)	44.0	2.97(-4)
12.0	1.36(-2)	1.06(-1)	1.99(-3)	5.36(-2)	6.61(-4)	44.5	2.54(-4)
12.5	8.75(-3)	8.68(-2)	1.05(-3)	3.90(-2)	2.69(-4)	45.0	2.17(-4)
13.0	5.44(-3)	6.99(-2)	5.30(-4)	2.76(-2)	1.02(-4)	45.5	1.86(-4)
13.5	3.28(-3)	5.54(-2)	2.56(-4)	1.90(-2)		46.0	1.58(-4)
14.0	1.91(-3)	4.33(-2)	1.19(-4)	1.27(-2)		46.5	1.35(-4)
14.5	1.08(-3)	3.33(-2)		8.25(-3)		47.0	1.15(-4)
15.0	5.87(-4)	2.53(-2)		5.20(-3)			
15.5	3.09(-4)	1.88(-2)		3.17(-3)			
16.0	1.57(-4)	1.38(-2)		1.87(-3)			
16.5		9.97(-3)		1.07(-3)			
17.0		7.07(-3)		5.86(-4)			
17.5		4.93(-3)		3.11(-4)			
18.0		3.38(-3)		1.59(-4)			
18.5		2.27(-3)					
19.0		1.50(-3)					
19.5		9.71(-4)					
20.0		6.17(-4)					
20.5		3.85(-4)					
21.0		2.35(-4)					
21.5		1.41(-4)					

TABLE 6. EXPOSURE TIMES FOR S-056 X-RAY PHOTOGRAPHS

MODE	FILTERS					
	1	2	3	4	5	6
Patrol Short	26	8.9	14.7	16.7	16.1	0.25
Patrol Normal	88	30	50	57	54	1
Patrol Long	287	97	161	184	175	2
Active (1, 2, or 3) Short	1.32	N/A	1.36	N/A	1.31	N/A
Active (1, 2, or 3) Normal	4.5	N/A	4.6	N/A	4.4	N/A
Active (1, 2, or 3) Long	14.4	N/A	14.7	N/A	14.2	N/A

Note: Exposure times given in seconds.

In the Patrol mode, used for routine observations, the camera was cycled once through each of the six filters for a total of six frames. The total time required for the sequence was approximately 1.8 min for Short (PS), 5 min for Normal (PN), and 15.5 min for Long (PL) exposures.

In the Active modes, used for studying bright regions that were evolving rapidly, the camera cycled through Filters 1, 3, and 5 in rapid succession, with the cycles being repeated a number of times over a period depending on which submode was chosen. The Active 1 mode required approximately 5 min for a complete sequence containing either 33 Short (A1S), 36 Normal (A1N), or 15 Long (A1L) exposures. The Active 2 mode (A2S, A2N, or A2L) required approximately 25 min for a complete sequence of 60 frames (20 at each of the 3 filters). The Active 3 mode (A3S, A3N, or A3L) required approximately 60 min for a complete sequence of 18 frames (6 at each of the 3 filters). In the Active 2 and 3 modes, the number of frames was the same for all choices of exposure times (Short, Normal, or Long).

The Auto mode (AUS, AUN, or AUL), used for flares or other transient phenomena, consisted of an Active 1 sequence, a 1-min delay, an Active 2 sequence, a 10-min delay, and an Active 3 sequence. However, the astronaut would often reinitiate the Auto mode several times rather than allow it to complete its prescribed exposure sequence to obtain more photographs during the flare.

The Single Frame mode (SFS, SFN, or SFL) allowed the astronaut to select a particular filter to obtain a single photograph. The exposure time was the same as that filter would have had in the Patrol mode.

An additional mode, called the Super-Long mode (S^L), was devised after the first manned mission to allow exposures of arbitrary length. This mode was usually effected by the astronaut selecting the desired filter and the Single Frame mode (although other modes could be used), initiating the camera operation, turning off the camera power while the shutter was open, waiting the desired length of time, turning on the power, and terminating the operation. The Super-Long frames are easily identified by the fact that the data block light array is split into two sections, with the exposure stop-time information separated from the rest of the array. Each Super-Long frame usually contains a primary image of long duration and a secondary image exposed just before termination of the operation. Sometimes there is more than one secondary image. More details, including an example of a Super-Long frame, are given by Wilson [2].

C. Films and Calibration

This section discusses the various films used, both originals and copies, and their calibration. Calibration is based on sensitometry performed on samples of the flight film. The method of obtaining the sensitometric data, reducing it, and obtaining the final film characteristic curves is described in "Film Calibration for the Skylab ATM/S-056 X-Ray Telescope," to be published in 1977.

1. Film Description—Originals and Copies. Five rolls (or loads) of 35 mm film were exposed during the three manned Skylab missions, four of black-and-white emulsion and one of color reversal emulsion. Each of these rolls of film is referred to as the flight film, the original, or the first-generation film. Information concerning the usage of the film is given in Table 7. (Note that Load 5, the color film, was exposed before Load 4.)

The black-and-white film was Kodak SO-212, a film developed especially for this experiment with an emulsion similar to Kodak Panatomic-X aerial film Type 3400 but without the protective gelatin overcoat and with a Rem-Jet anti-static backing. The color film was Kodak SO-242, an aerial color reversal film with slightly better resolution but slower speed than SO-212. A feature of the SO-242 is that it shows spectral sensitivity to X-rays. Due to the wavelength

TABLE 7. S-056 FILM USAGE

MISSION	LOAD	FILM TYPE	DATES	DAY OF YEAR	FRAMES USED
SL2	1	S0-212 (B&W)	29 May 1973 - 18 Jun 1973	149 to 169	3998
SL3	2	S0-212 (B&W)	07 Aug 1973 - 24 Aug 1973	219 to 236	5653
	3	S0-212 (B&W)	24 Aug 1973 - 21 Sep 1973	236 to 264	5797
SL4	5	S0-242 (Color)	26 Nov 1973 - 25 Dec 1973	330 to 359	5029
	4	S0-212 (B&W)	26 Dec 1973 - 03 Feb 1974	360 to 34	6713
					TOTAL 27 190

variation of the absorption by the emulsion, X-rays of different wavelength penetrate to different emulsion layers and thus appear as different colors on the developed film. Therefore, it may be possible to extract spectral information by color densitometry of color copies.

Copies have been prepared of the original film for submission to the NSSDC and for routine use, including densitometry. The film used for second-generation (positive) copies of the black-and-white film (Loads 1 through 4) was Kodak Type 5235, a panchromatic separation film. To reproduce the large dynamic range on the originals (with densities up to almost 4.0), a high-exposure copy for bright X-ray features and a low-exposure copy for faint features were required. These two different exposure copies are therefore known as bright-feature and faint-feature versions. The two copies also differ in the contrast (γ) to which they were developed. The bright-feature copy has $\gamma \approx 0.7$, while the faint-feature copy has $\gamma \approx 1.0$.

Both black-and-white and color copies have been made of the color film (Load 5). Because the flight or first-generation film was a color reversal film, the second-generation black-and-white copies are negative copies. Again, both bright-feature and faint-feature versions were made. The copy film was Kodak Type 2402, a Plus-X aerographic film with a panchromatic emulsion having extended red sensitivity. Third-generation positive copies were then made on Kodak Type 5366, a duplicating positive film. The third-generation copies were normally exposed copies of each of the bright- and faint-feature versions of the second-generation films. It is these black-and-white positive third-generation copies of Load 5, in both the bright-feature and faint-feature versions, that have been sent to the NSSDC.

In addition to the black-and-white copies of Load 5 mentioned previously, color copies and color-separation copies have been made for use at the experimenters' own institutions. The second-generation color copies were made on Kodak Type 5389, an Ektachrome R color reversal print film. The second-generation color-separation copies are black-and-white negatives made on Kodak Type 5234, a duplicating panchromatic negative film; three separate copies were made with cyan, yellow, and magenta filters.

2. Format of Film Sensitometry. For calibration, each load of film contains sets of sensitometric exposures at both the beginning and the end of the film. The beginning of the film is known as the "Heads," while the end is known as the "Tails." The order of occurrence of the solar images goes from Heads to Tails; i. e., the first or earliest images are closest to the Heads end and the last or latest exposures are closest to the Tails end. To allow users to verify the orientation of any one film and to find the "standard" sensitometry set as described later, Tables 8 through 12 identify each set for each load. The tables show the order in which the sets are present and give considerable information about each set.

The X-ray sensitometry, which was the only kind actually used for calibration, was provided by Sperry Support Services (Sperry Rand Corporation) and The Aerospace Corporation. Aluminum, titanium, and copper sources were used. Sperry also provided visible light and ultraviolet sensitometry. The photographic white-light wedges, used to monitor changes in film properties, were exposed by the NASA/Johnson Space Center (JSC). The appearance of a typical step for each type of sensitometry is shown in Figure 8.

3. Calibration Data. The film calibration information is summarized in Table 13 which relates the exposure in photons cm^{-2} to step number in a selected "standard" sensitometry set for each load of film. Note that use of the table does not depend on the particular copy of a load of film that is being used.

The standard sensitometry sets are all Sperry X-ray sets and can be found with the aid of Tables 8 through 12. Set 106 on Load 1 is the fourth set from the Heads end of the film; it is surrounded by the shadows of two trapezoidal pieces of tape on the flight film. Set 047-I on Load 2 is the fifth set from the Heads end of the film and is the first X-ray set on the Heads end. Set 048-I on Load 3 is also the fifth set from the Heads end and the first X-ray set on the film. Set 256 on Load 4 is the first set immediately following the two JSC white light photographic wedges which follow the solar images on the Tails end of the film. Set 253 on Load 5 is the Sperry X-ray set that is immediately in front of the Aerospace sensitometry on the Tails end of the film.

TABLE 8. LOAD 1, IDENTIFICATION OF SENSITOMETRY SETS

ORIGIN OF SENSITOMETRY SET	TYPE OF SENSITOMETRY	PRE OR POST FLIGHT	SOURCE OR λ (A)	SET NO	END OF SET WITH HIGH EXPOSURES	NUMBER OF STEPS (INTENDED OR ACTUAL)	REMARKS, STEP SIZE, OTHER FEATURES ON FILM
↑ HEADS END							
Sperry	X-Ray	Post	T1	109	H	21	Each step 5/16 in wide (along film), 1 1/2 in from center to center
Sperry	X-Ray	Post	T1	108	H	22	Same as Set 109
Sperry	X-Ray	Post	A1	107	H	21	Same as Set 109
Sperry	X-Ray	Post	A1	106	H	21	□ Trapezoidal piece of tape on flight film Same as Set 109
Sperry	Visible	Post	6400		T	21	□ Trapezoidal piece of tape on flight film 1 1/4 in wide gate (highly exposed) Each step 3/8 to 1/2 in wide, 5/8 in from center to center
Sperry	Visible	Post	5200		T	21	Same as λ 6400
Sperry	Visible	Post	4000		T	21	Same as λ 6400
Sperry	UV	Post	2600		T	21	1-in-wide gate (highly exposed) Same as λ 6400
Aerospace	X-Ray	Post	A1		T	28	
Aerospace	X-Ray	Post	Cu		T	15	
JSC	Photo	Pre	WL	1	T		15 3/4 in. highly exposed section
JSC	Photo	Pre	WL	2	T		Tick mark tenth step from Tails
Sperry	UV	Pre	2600		H	21	Each step 3/8 to 7/16 in wide, 5/8 in from center to center
Sperry	Visible	Pre	4000		H	21	Same as λ 2600
Sperry	Visible	Pre	5200		H	21	Same as λ 2600
Sperry	Visible	Pre	6400		H	21	Same as λ 2600
Sperry	X-Ray	Pre	A1	1	T	27	Each step 5/16 in wide, 1 1/2 in from center to center, some overlapping steps
Sperry	X-Ray	Pre	T1	2	T	24	Same step size and spacing as Set 1
Sperry	X-Ray	Pre	A1	3	T	24	Same as Set 2
Sperry	X-Ray	Pre	T1	4	T	23	Same as Set 2
SOLAR IMAGES							
JSC	Photo	Post	WL	3	T		
JSC	Photo	Post	WL	4	T		
↓ TAILS END							

H = Heads, T = Tails, WL = White Light, UV = Ultraviolet Light, Photo = Photographic

REPRODUCIBILITY OF THE
ORIGINAL PAGE IS POOR

TABLE 9. LOAD 2, IDENTIFICATION OF SENSITOMETRY SETS

TABLE 10. LOAD 3, IDENTIFICATION OF SENSITOMETRY SETS

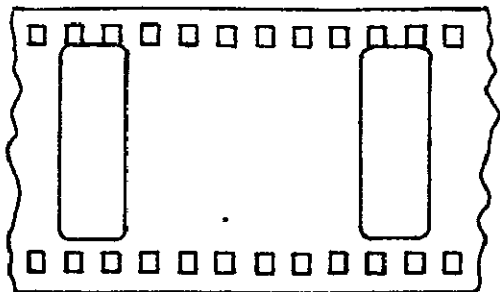
ORIGIN OF SENSITOMETRY SET	TYPE OF SENSITOMETRY	PRE OR POST FLIGHT	SOURCE OR λ (A)	SET NO	END OF SET WITH HIGH EXPOSURES	NUMBER OF STEPS (INTENDED OR ACTUAL)	REMARKS, STEP SIZE, OTHER FEATURES ON FILM
↑ HEADS END							
Sperry	UV	Pre	2600		H	21	Each step 3/8 to 1/16 in wide, 5/8 in from center to center 1 in wide gate (highly exposed)
Sperry	Visible	Pre	4000		H	21	Same as λ 2600
Sperry	Visible	Pre	5200		H	21	Same as λ 2600
Sperry	Visible	Pre	6400		H	21	Same as λ 2600 1 1/2 in wide gate (?)
Sperry	X-Ray	Pre	A1	048-I	T	22	Each step 5/16 in wide, 1 1/2 in from center to center
Sperry	X-Ray	Pre	A1	048-II	T	20	Same as Set 048-I ~2 1/4 in highly exposed section, 1/2 in splice
JSC	Photo	Pre	WL	1	T		
JSC	Photo	Pre	WL	2	T		
SOLAR IMAGES							
JSC	Photo	Post	WL	3	T		
JSC	Photo	Post	WL	4	T		
Sperry	X-Ray	Post	A1	166	T	21	1/2 in wide splice, 1 in wide gate Each step 5/16 in wide, 5/8 in, normal from center to center, many steps touching
Sperry	X-Ray	Post	T1	167	T	9	Same step size, normal spacing as Set 166 1 in wide gate
Sperry	UV	Post	2600		H	21	Each step 3/8 to 7/16 in wide, 5/8 in total spacing
Sperry	Visible	Post	4000		H	21	Same as λ 2600
Sperry	Visible	Post	5200		H	21	Same as λ 2600
Sperry	Visible	Post	6400		H	21	Same as λ 2600 1 in wide gate, 1/2 in splice, 1/2 in splice Messed up, steps overlapping
↓ TAILS END							

TABLE 11. LOAD 4, IDENTIFICATION OF SENSITOMETRY SETS

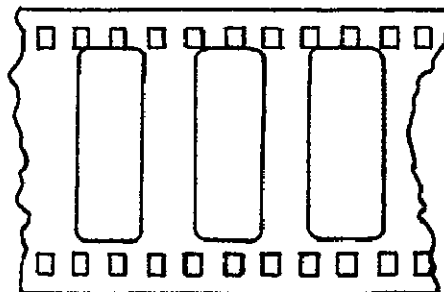
TABLE 12. LOAD 5, IDENTIFICATION OF SENSITOMETRY SETS

ORIGIN OF SENSITOMETRY SET	TYPE OF SENSITOMETRY	PRE OR POST FLIGHT	SOURCE OR λ (A)	SET NO	END OF SET WITH HIGH EXPOSURES	NUMBER OF STEPS (INTENDED OR ACTUAL)	REMARKS, STEP SIZE, OTHER FEATURES ON FILM
↑ HEADS END							
JSC	Photo	Pre	WL	1	T		
JSC	Photo	Pre	WL	2	T		
SOLAR IMAGES							
JSC	Photo	Post	WL	3	T		
JSC	Photo	Post	WL	4	T		
Sperry	Visible	Post	6400		T	21	1/2 in wide splice, "Marshall Sensi", highly exposed mark (made by tape on flight film), 1 in wide gate Each step 3/8 to 7/16 in wide, 5/8 in from center to center
Sperry	Visible	Post	5200		T	21	Same as λ 6400
Sperry	Visible	Post	4000		T	21	Same as λ 6400
Sperry	UV	Post	2600		T	21	Same as λ 6400
Sperry	X-Ray	Post	T1	255	H	22	1 in wide gate Each step 5/16 in wide, 1 1/2 in from center to center
Sperry	X-Ray	Post	Cu	254	H	22	Same as Set 255
Sperry	X-Ray	Post	A1	253	H	21	Same as Set 255
Aerospace	X-Ray	Post	A1	1	T	21	1 in wide gate, 10 in highly exposed section, 1/2 in wide splice, "Aerospace Sensi"
Aerospace	X-Ray	Post	Cu	2	T	18	
Aerospace	X-Ray	Post	Cu	3	T	13	
							2 1/2 in long, medium exposed section, 1/2 in wide splice, "227"
Sperry	X-Ray	Test	A1	227	H	12	
Sperry	X-Ray	Test	A1	226	H	12	1/2 in wide splice, "226"
↓ TAILS END							

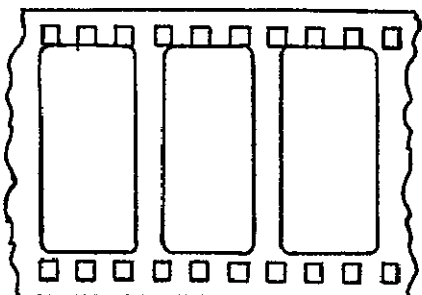
Test = Sensitometry set made on film which did not fly on Skylab



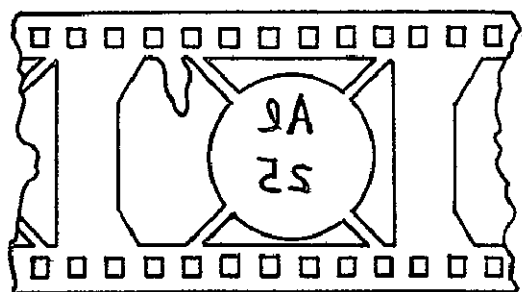
SPERRY X-RAY
LOADS 1,4,5 - ALL
LOADS 2,3 - PREFLIGHT ONLY



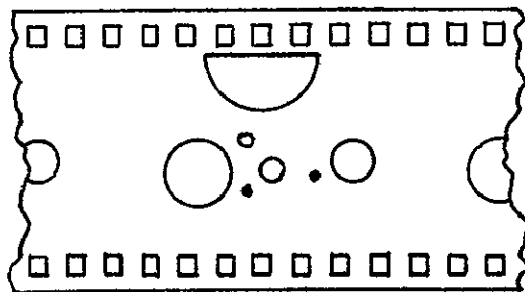
SPERRY X-RAY
LOADS 2,3 - POSTFLIGHT ONLY



SPERRY VISIBLE, UV
ALL LOADS



AEROSPACE X-RAY
LOAD 1



AEROSPACE X-RAY
LOADS 2,3,4,5

EMULSION IS DOWN ON FLIGHT FILM AND THIRD-GENERATION COPY, UP
ON SECOND-GENERATION COPY. TAILS IS TO THE RIGHT IN ALL CASES
EXCEPT AEROSPACE X-RAY LOAD 4 WHERE HEADS IS TO THE RIGHT.

Figure 8. Appearance of typical sensitometry sets.

TABLE 13. S-056 FILM CALIBRATION

STEP NO. FROM HIGH EXPOSURE END	EXPOSURE (photon cm ⁻²)				
	LOAD 1 SET 106	LOAD 2 SET 047-I	LOAD 3 SET 048-I	LOAD 4 SET 256	LOAD 5 SET 253
	↑ HEADS	↑ TAILS	↑ TAILS	↑ TAILS	↑ HEADS
1	5.97(10)	3.05(10)	4.06(10)	3.31(11)	1.30(11)
2	2.99(10)	1.81(10)	2.10(10)	1.66(11)	6.49(10)
3	1.49(10)	8.99(9)	9.62(9)	8.28(10)	3.24(10)
4	7.46(9)	4.12(9)	4.79(9)	4.14(10)	1.62(10)
5	3.76(9)	2.15(9)	2.40(9)	2.07(10)	8.11(9)
6	1.81(9)	1.05(9)	1.15(9)	1.04(10)	4.06(9)
7	1.38(9)	7.38(8)	8.26(8)	4.97(9)	2.87(9)
8	9.29(8)	5.22(8)	5.89(8)	3.64(9)	1.97(9)
9	6.53(8)	3.76(8)	4.09(8)	2.50(9)	1.39(9)
10	4.65(8)	2.62(8)	2.91(8)	1.72(9)	9.93(8)
11	3.27(8)	1.85(8)	2.06(8)	1.22(9)	6.98(8)
12	2.32(8)	1.31(8)	1.46(8)	8.55(8)	4.97(8)
13	1.67(8)	9.40(7)	1.05(8)	6.08(8)	3.56(8)
14	1.16(8)	6.53(7)	7.31(7)	4.40(8)	2.48(8)
15	7.98(7)	4.49(7)	5.04(7)	3.10(8)	1.71(8)
16	5.81(7)	3.27(7)	3.66(7)	2.15(8)	1.24(8)
17	4.36(7)	2.92(7)	2.74(7)	1.57(8)	9.31(7)
18	2.90(7)	2.60(7)	1.83(7)	1.17(8)	6.21(7)
19	2.18(7)	1.22(7)	1.37(7)	7.82(7)	4.66(7)
20	1.45(7)	8.17(6)	9.14(6)	5.87(7)	3.10(7)
21	7.26(6)	4.08(6)	9.14(6)	3.91(7)	1.55(7)
22			4.57(6)	1.95(7)	
	↓ TAILS	↓ HEADS	↓ HEADS	↓ HEADS	↓ TAILS

The step numbers within each set begin at the end with the highest exposure steps, i.e., the steps which are most different from the background. The central portion of each step should be used for density measurements.

D. Solar Observations and Ancillary Data

The S-056 X-ray telescope obtained over 27 000 photographs (filter-heliograms) of the Sun during the Skylab mission. Each frame normally consists of an image of the Sun plus the image of the data block lights used to identify the instrumental parameters associated with that exposure. Often the solar image will show only active regions; the limb and the orientation are not always obvious. However, the visible light images (Filter 6) show the entire disk and are often an aid in identifying when the telescope was in a Patrol mode and thus the sequencing of all of the filters in the Patrol mode.

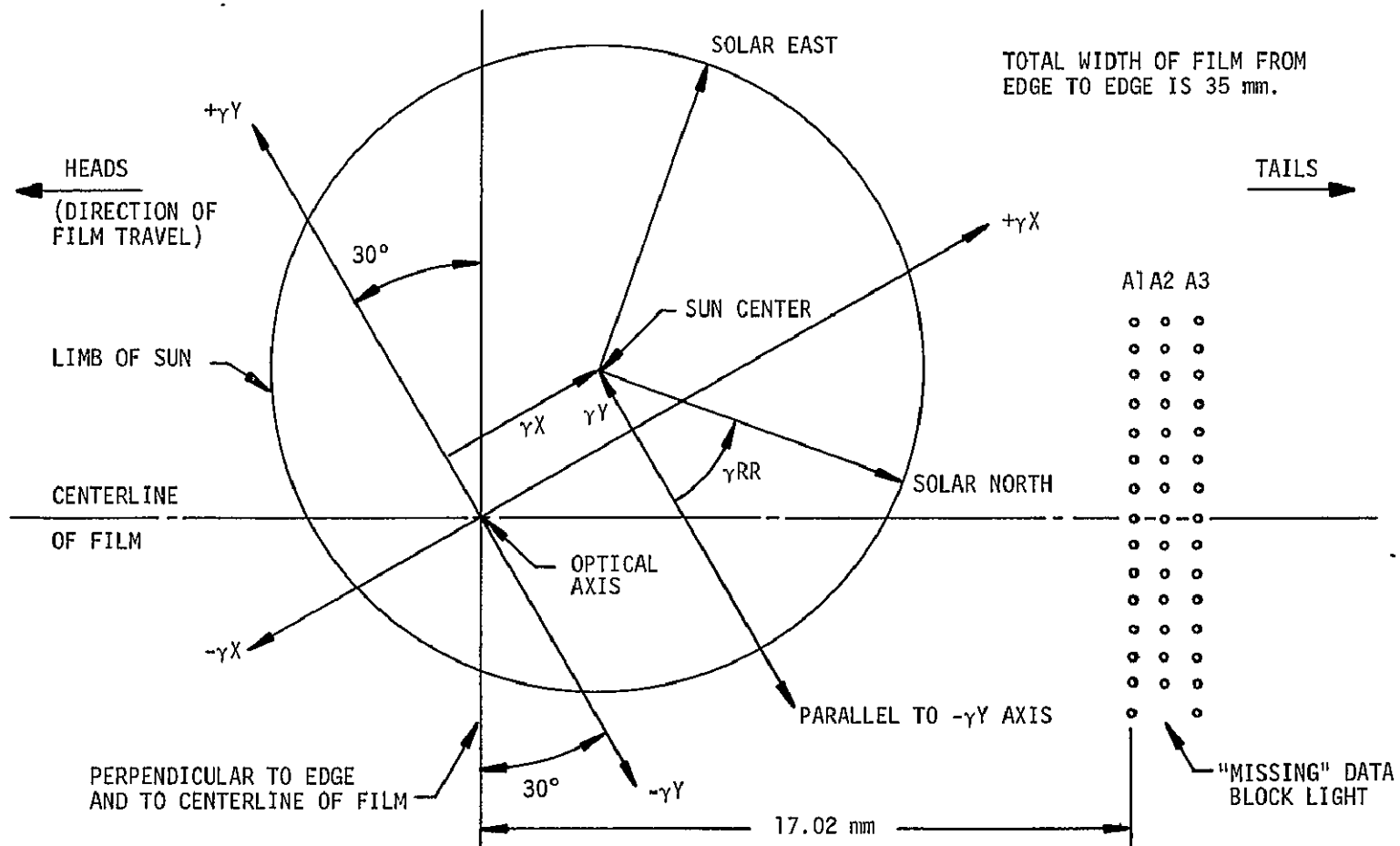
The remainder of this section will describe listings of the S-056 frames, the position and orientation of the solar image on each frame, the data block lights and how to read them, and specialized catalogs containing information about observations of different types of solar features.

1. Frame Listings. The solar images were exposed on five loads of film. The number of frames and the time interval covered by each load are summarized in Table 7. Note that Load 5, the color film, was exposed before Load 4.

The data block images for all S-056 frames have been visually read and compiled in the "S-056 Frame Listing" (unpublished), a copy of which has been submitted to the NSSDC. In addition, the S-056 operations have been listed in the "ATM Mission Operation Log" [8], provided by Ball Brothers Research Corporation (BBRC), which identifies ATM experiment operations and gives positional reference information as a function of time during the Skylab missions. Because the Super-Long exposures were not made in a normal manner, only their start times appear in the BBRC publication. However, the "Atlas of Skylab ATM/S056 Super-Long Exposures and Stepped-Image Frames" [2] contains a listing of the 552 S-056 Super-Long mode operations that were performed during the last two manned missions and gives their exposure times.

2. Image Position and Orientation. Figure 9 illustrates the S-056 film format for normal images (if north is up, east is to the left). To use the figure, one should have the emulsion down on the flight film (also called first-generation) or on third-generation copies; the emulsion should be up on second-generation copies. Note that the position of the "missing" data block light

EMULSION DOWN ON FLIGHT FILM (FIRST GENERATION) AND THIRD-GENERATION COPY.
EMULSION UP ON SECOND-GENERATION COPY.



THE COORDINATES γX , γY , AND γRR ARE POSITIVE IN THE DIRECTION OF THE ARROWS. THE VALUES USED TO CONSTRUCT THE EXAMPLE SHOWN IN THE FIGURE ARE $\gamma X = +500$ (arc s), $\gamma Y = +200$ (arc s), AND $\gamma RR = +2,400$ (arc min). NOTE THAT FOR γX AND γY , 100 arc s = 0.923 mm.

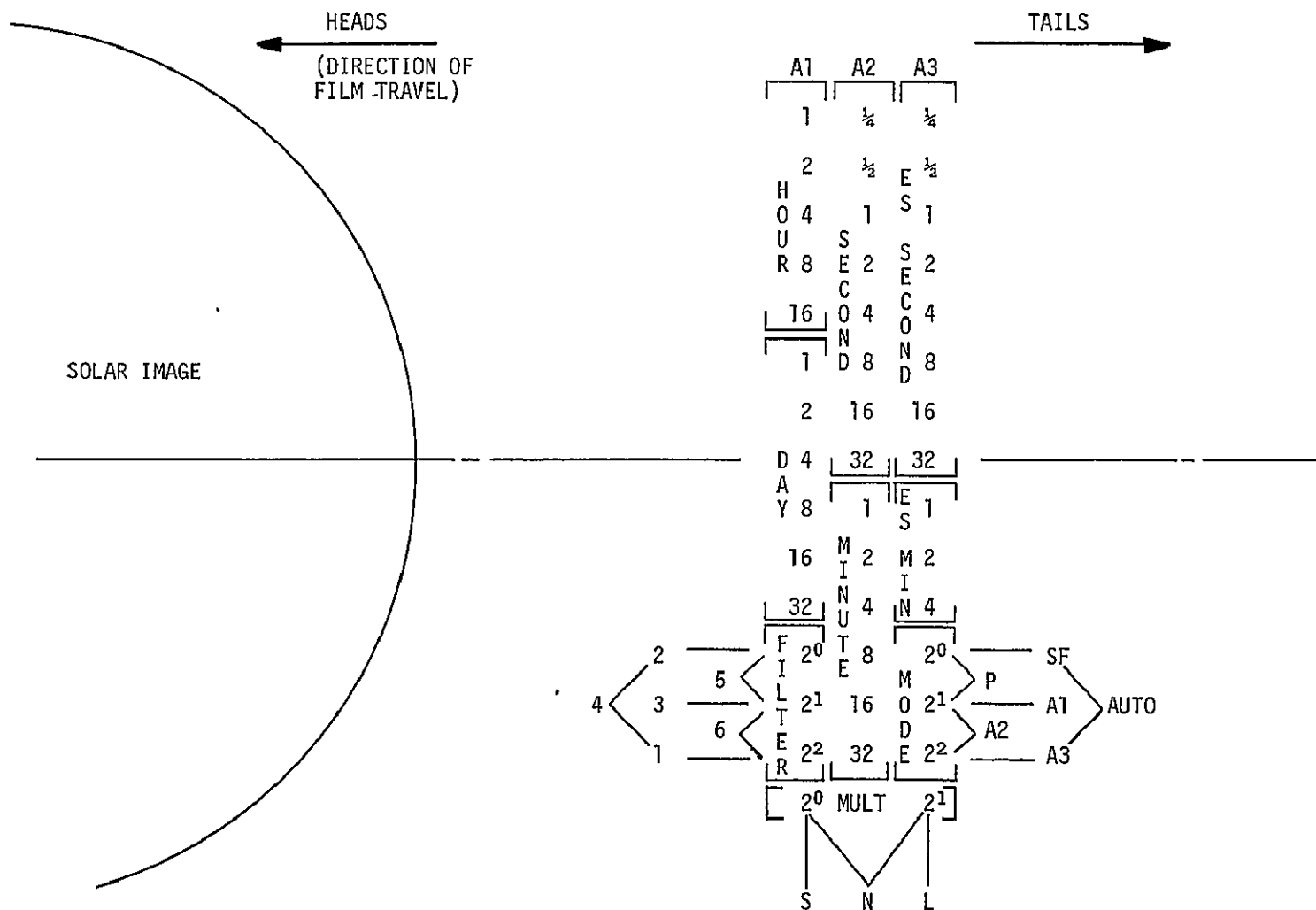
Figure 9. Format of S-056 frame.

(which may have to be determined from other nearby frames) can sometimes be helpful in orienting the film. The intersection of the telescope optical axis with the film plane is on the centerline of the film and is 17.02 mm in the direction of the Heads end from the A1 column of data block lights for that frame. Sometimes the film did not advance properly and the solar image is superimposed on the data block lights for the preceding frame.

ATM experiment pointing was provided by the experiment pointing control, which used the fine Sun sensor as reference and fine-pointed the ATM canister with an accuracy and stability of better than 2.5 arc s. The offsets from Sun center (given by the angles γ_X and γ_Y) were accomplished by means of actuators at the canister gimbal pivots and the canister roll positioning (given by the angle γ_{RR}) by the roll position mechanism; both were operated from the ATM control and display panel. The values of γ_{RR} , γ_X , and γ_Y as a function of time are tabulated in the BBRC "ATM Mission Operation Log" [8]. The value of λ_{RR} is given in arc min; γ_X and γ_Y are given in arc s. The accuracy of the roll angles reconstructed from computer records has been questioned because of disagreements with other determinations, such as those based on star fields observed by the High Altitude Observatory S-052 White Light Coronagraph. Further discussions of this question and the ATM Experiment Pointing System in general can be found in BBRC technical reports [9,10]. Of course, in the comparison of images obtained during a period when the roll angle was not changed, knowledge of the exact value of the roll angle often is not required.

To find the center of the Sun and the direction of solar north on an S-056 frame from given values of γ_X , γ_Y , and γ_{RR} , one should proceed as follows (Fig. 9). First, find the center of the Sun by converting γ_X and γ_Y from arc seconds to millimeters using the plate scale of 9.23×10^{-3} mm/arc s and then shifting from the optical axis by those amounts along the appropriate directions as shown in the figure. Then find solar north by going counterclockwise, for positive γ_{RR} in arc minutes, from the negative γ_Y direction. The offset of the γ_Y axis by 30 degrees from the perpendicular to the edge of the film is caused by the orientation of the film magazine within the S-056 instrument and the ATM canister.

3. Data Block Lights. To identify each exposure on the film, a data block system was provided, consisting of 44 subminiature lamps whose images were projected onto the film. These data block images identified the camera mode of operation, exposure multiplier (i.e., whether the exposure was Short, Normal, or Long), filter, exposure start time, and exposure stop time. Figure 10 illustrates the data block configuration and deciphers the code for the various times, modes, filters, and multipliers (Short, Normal, or Long), indicated by



EMULSION IS DOWN ON FLIGHT FILM. THERE IS NO DATA BLOCK LIGHT IN THE BOTTOM ROW OF COLUMN "A2".

Figure 10. Data block configuration.

the appropriately lit data lights. The middle column has only 14 lights instead of 15; noting the position of the missing step is often an aid in orienting the data block lights and the solar image. While time of exposure start and stop was reckoned from the onboard spacecraft clock, the individual mode exposures were controlled internally by the experiment's camera/thermal control electronics package. The exposure start time was encoded on the film in the A1 and A2 columns when the astronaut initiated the operation. Similarly, the exposure stop time (in minutes, modulo 8, and seconds only) was encoded in the A3 column when the operation was terminated. Exposure time or duration is directly calculated as the difference between exposure start time and exposure stop time.

The "Day" information (Fig. 10) refers to the spacecraft "clock day," which recycled every 64 days. Table 14 correlates the day-of-year (DOY) and the date (DATE), mission day (MD), and clock day (CD) during the Skylab missions and provides additional information such as the 6 h periods of each day for which microfilm is available, extravehicular activity (EVA) occurrences, and mission milestones.

4. Specialized Catalogs. The S-056 film and operations logs have been examined for evidence of various solar features. Some of the results have been compiled and published in two different forms. The "Compilation of Flares and Transients Observed by the S-056 Solar X-Ray Telescope during the Skylab Missions" [4] contains a list of flares and transients observed by the S-056 telescope together with the time that S-056 observations of that event began. Individual frames are not listed.

The "Atlas of Skylab ATM/S056 Coronal Hole Observations" [5] contains a list of all Patrol Long and Single Frame Long Filter 3 frames taken during the first two manned missions (Loads 1, 2, and 3). These frames, together with the Super-Long frames listed by Wilson [2], represent the best opportunity for detection of coronal holes by the S-056 telescope; however, not all of them necessarily show the presence of coronal holes.

E. Telescope Housekeeping Data (Microfilm Records)

The S-056 housekeeping data consist of current, temperature, and discrete event measurements. Five hundred and sixty-five microfilm records of these data have been submitted to the NSSDC, each record representing a 6 h time period. Table 14 identifies all of the 6 h periods for which microfilm records are available. Because the thermal control system functioned properly

TABLE 14. CORRELATION BETWEEN DATE AND VARIOUS "DAYS,"
 MICROFILM AVAILABILITY FOR 6 h PERIODS,
 MISSION MILESTONES

DOY	DATE	MD	CD	MICROFILM	REMARKS
132	5/12				
133	5/13				
134	5/14		0		
135	5/15		1		
136	5/16		2		
137	5/17		3		
138	5/18		4		
139	5/19		5		
140	5/20		6		
141	5/21		7		
142	5/22		8		
143	5/23		9		
144	5/24		10		
145	5/25	1	11		
146	5/26	2	12		
147	5/27	3	13		
148	5/28	4	14		
149	5/29	5	15		
150	5/30	6	16	1 2 3 4	
151	5/31	7	17	1 3 4	
152	6/1	8	18	1 3 4	
153	6/2	9	19	1 3 4	
154	6/3	10	20	1 3 4	
155	6/4	11	21	1 3 4	
156	6/5	12	22	1 3 4	
157	6/6	13	23	1 3 4	
158	6/7	14	24	1 2 3 4	
159	6/8	15	25	1 3 4	
160	6/9	16	26	1 3 4	
161	6/10	17	27	1 3 4	
162	6/11	18	28	1 3 4	
163	6/12	19	29	1 2 3 4	
164	6/13	20	30	1 2 3 4	
165	6/14	21	31	1 2 3 4	
166	6/15	22	32	1 2 3 4	
167	6/16	23	33	1 2 3 4	
168	6/17	24	34	1 2 3 4	
169	6/18	25	35	1 2 3 4	
170	6/19	26	36		EVA
171	6/20	27	37		
172	6/21	28	38		
173	6/22	29	39		Splashdown SL2
174	6/23		40		
175	6/24		41		
176	6/25		42		
177	6/26		43		
178	6/27		44		
179	6/28		45		
180	6/29		46		
181	6/30		47		
182	7/1		48		
183	7/2		49		
184	7/3		50		
185	7/4		51		
186	7/5		52		
187	7/6		53		
188	7/7		54		
189	7/8		55		
190	7/9		56		
191	7/10		57		

TABLE 14. (Continued)

DOY	DATE	MD	CD	MICROFILM	REMARKS
192	7/11			58	
193	7/12			59	
194	7/13			60	
195	7/14			61	
196	7/15			62	
197	7/16			63	
198	7/17			0	
199	7/18			1	
200	7/19			2	
201	7/20			3	
202	7/21			4	
203	7/22			5	
204	7/23			6	
205	7/24			7	
206	7/25			8	
207	7/26			9	
208	7/27			10	
209	7/28	1	11	1 2 3	
210	7/29	2	12	1 2 3 4	Launch SL3
211	7/30	3	13	1 3 4	
212	7/31	4	14	1 2 3 4	
213	8/1	5	15	1 3 4	
214	8/2	6	16	1 3 4	
215	8/3	7	17	1 3	
216	8/4	8	18	1 2	
217	8/5	9	19	3 4	
218	8/6	10	20	1 2 3 4	
219	8/7	11	21	1 2 3 4	
220	8/8	12	22	1 2 3 4	Harvard Rocket
221	8/9	13	23	1 2 3 4	
222	8/10	14	24	1 2 3 4	
223	8/11	15	25	1 2 3 4	
224	8/12	16	26	1 2 3 4	
225	8/13	17	27	1 2 3 4	
226	8/14	18	28	1 2 3 4	
227	8/15	19	29	1 2 3 4	
228	8/16	20	30	1 2 3 4	
229	8/17	21	31	1 2 3 4	
230	8/18	22	32	1 2 3 4	
231	8/19	23	33	1 2 3 4	
232	8/20	24	34	1 2 3 4	EVA
233	8/21	25	35	1 2 3 4	
234	8/22	26	36	1 2 3 4	
235	8/23	27	37	1 2 3 4	
236	8/24	28	38	1 2 3 4	
237	8/25	29	39	1 2 3 4	
238	8/26	30	40	1 2 3 4	
239	8/27	31	41	1 2 3 4	
240	8/28	32	42	1 2 3 4	
241	8/29	33	43	1 2 3 4	
242	8/30	34	44	1 2 3 4	Colorado Rocket
243	8/31	35	45	1 2 3 4	
244	9/1	36	46	1 2 3 4	
245	9/2	37	47	1 2 3 4	
246	9/3	38	48	1 2 3 4	
247	9/4	39	49	1 2 3 4	
248	9/5	40	50	1 2 3 4	NRL Rocket
249	9/6	41	51	1 2 3 4	
250	9/7	42	52	1 2 3 4	
251	9/8	43	53	1 2 3 4	

TABLE 14. (Continued)

DOY	DATE	MD	CD	MICROFILM	REMARKS
252	9/9	44	54	1 2 3 4	
253	9/10	45	55	1 2 3 4	
254	9/11	46	56	1 2 3 4	
255	9/12	47	57	1 2 3 4	
256	9/13	48	58	1 2 3 4	
257	9/14	49	59	1 2 3 4	
258	9/15	50	60	1 2 3 4	
259	9/16	51	61	1 2 3 4	
260	9/17	52	62	1 2 3 4	
261	9/18	53	63	1 2 3 4	
262	9/19	54	0	1 2 3 4	
263	9/20	55	1	1 2 3 4	SCO X-1 Observation
264	9/21	56	2	1 2 3 4	
265	9/22	57	3	1 2 3 4	EVA
266	9/23	58	4		
267	9/24	59	5		
268	9/25	60	6		Splashdown SL3
269	9/26		7		
270	9/27		8		
271	9/28		9		
272	9/29		10		
273	9/30		11		
274	10/1		12		
275	10/2		13		
276	10/3		14		
277	10/4		15		
278	10/5		16		
279	10/6		17		
280	10/7		18		
281	10/8		19		
282	10/9		20		
283	10/10		21		
284	10/11		22		
285	10/12		23		
286	10/13		24		
287	10/14		25		
288	10/15		26		
289	10/16		27		
290	10/17		28		
291	10/18		29		
292	10/19		30		
293	10/20		31		
294	10/21		32		
295	10/22		33		
296	10/23		34		
297	10/24		35		
298	10/25		36		
299	10/26		37		
300	10/27		38		
301	10/28		39		
302	10/29		40		
303	10/30		41		
304	10/31		42		
305	11/1		43		
306	11/2		44		
307	11/3		45		
308	11/4		46		
309	11/5		47		

TABLE 14. (Continued)

DOY	DATE	MD	CD	MICROFILM	REMARKS
310	11/6		48		Mercury Transit
311	11/7		49		
312	11/8		50		
313	11/9		51		
314	11/10		52		
315	11/11		53		
316	11/12		54		
317	11/13		55		
318	11/14		56		
319	11/15		57		
320	11/16	1	58		Launch SL4
321	11/17	2	59		
322	11/18	3	60		
323	11/19	4	61		
324	11/20	5	62		
325	11/21	6	63		EVA
326	11/22	7	0		
327	11/23	8	1		
328	11/24	9	2		
329	11/25	10	3		
330	11/26	11	4	4	Leicester Rocket
331	11/27	12	5	1 2 3 4	
332	11/28	13	6	1 2 3 4	
333	11/29	14	7	1 2 3 4	
334	11/30	15	8	1 2 3 4	
335	12/1	16	9	1 2 3 4	Harvard Rocket
336	12/2	17	10	1 2 3 4	
337	12/3	18	11	1 2 3 4	
338	12/4	19	12	1 2 3 4	
339	12/5	20	13	1 2 3 4	
340	12/6	21	14	1 2 3 4	Lockheed Rocket
341	12/7	22	15	1 2 3 4	
342	12/8	23	16	1 2 3 4	
343	12/9	24	17	1 2 3 4	
344	12/10	25	18	1 2 3 4	
345	12/11	26	19	1 2 3 4	Solar Eclipse
346	12/12	27	20	1 2 3 4	
347	12/13	28	21	1 2 3 4	
348	12/14	29	22	1 2 3 4	
349	12/15	30	23	1 2 3 4	
350	12/16	31	24	1 2 3 4	EVA
351	12/17	32	25	1 2 3 4	
352	12/18	33	26	1 2 3 4	
353	12/19	34	27	1 2 3 4	
354	12/20	35	28	1 2 3 4	
355	12/21	36	29	1 2 3 4	EVA
356	12/22	37	30	1 2 3 4	
357	12/23	38	31	1 2 3 4	
358	12/24	39	32	1 2 3 4	
359	12/25	40	33	1 2 3 4	
360	12/26	41	34	1 2 3 4	EVA
361	12/27	42	35	1 2 3 4	
362	12/28	43	36	1 2 3 4	
363	12/29	44	37	1 2 3 4	
364	12/30	45	38	1 2 3 4	
365	12/31	46	39	1 2 3 4	
1	1/1	47	40	1 2 3 4	
2	1/2	48	41	1 2 3 4	
3	1/3	49	42	1 2 3 4	
4	1/4	50	43	1 2 3 4	

TABLE 14. (Concluded)

DOY	DATE	MD	CD	MICROFILM	REMARKS
5	1/5	51	44	1 2 3 4	
6	1/6	52	45	1 2 3 4	
7	1/7	53	46	1 2 3 4	
8	1/8	54	47	1 2 3 4	
9	1/9	55	48	1 2 3 4	
10	1/10	56	49	1 2 3 4	
11	1/11	57	50	1 2 3 4	
12	1/12	58	51	1 2 3 4	
13	1/13	59	52	1 2 3 4	
14	1/14	60	53	1 2 3 4	
15	1/15	61	54	1 2 3 4	
16	1/16	62	55	1 2 3 4	
17	1/17	63	56	1 2 3 4	
18	1/18	64	57	1 2 3 4	
19	1/19	65	58	1 2 3 4	
20	1/20	66	59	1 2 3 4	
21	1/21	67	60	1 2 3 4	
22	1/22	68	61	1 2 3 4	Aerospace Rocket
23	1/23	69	62	1 2 3 4	
24	1/24	70	63	1 2 3 4	
25	1/25	71	0	1 2 3 4	
26	1/26	72	1	1 2 3 4	
27	1/27	73	2	1 2 3 4	
28	1/28	74	3	1 2 3 4	
29	1/29	75	4	1 2 3 4	
30	1/30	76	5	1 2 3 4	
31	1/31	77	6	1 2 3 4	
32	2/1	78	7	1 2 3 4	
33	2/2	79	8	1 2 3 4	
34	2/3	80	9	1 3	EVA
35	2/4	81	10		
36	2/5	82	11	3	
37	2/6	83	12		
38	2/7	84	13		
39	2/8	85	14		Splashdown SL4
40	2/9		15		
41	2/10		16		
42	2/11		17		
43	2/12		18		
44	2/13		19		
45	2/14		20		
46	2/15		21		
47	2/16		22		
48	2/17		23		
49	2/18		24		
50	2/19		25		
51	2/20		26		
52	2/21		27		
53	2/22		28		
54	2/23		29		

and all current measurements were within the allowable range, users will not normally need the temperature and current data. However, because the data are available on the microfilm, they will be described briefly here. The discrete event data are potentially more useful although, again, most users will not need the information.

Nine temperatures and five currents were measured to monitor instrument temperatures and certain S-056 operations. Table 15 identifies these measurements and gives pertinent information about them. The temperature and current data were telemetered in real time only and thus are available only for those times when Skylab was in range of a ground station. No provision was made for recording the data for later transmission. Five discrete event measurements were monitored; these are identified in Table 16. The discrete event data were both telemetered in real time and recorded for later transmission; they are thus much more complete than the temperature and current data. Occasionally, data dropouts occurred, resulting in the permanent loss of some data.

TABLE 15. TEMPERATURE AND CURRENT MEASUREMENTS

MEASUREMENT NUMBER	PARAMETER	OPERATING RANGE NORMAL ALLOWABLE		SIGNIFICANCE OF NORMAL READING
C036	Temperature, X-REA 1	68 to 80°F	32 to 104°F	Proper operation of the X-REA power supply in the area of the power supply filter
C037	Temperature, Camera Electronics Package	67 to 69°F	32 to 104°F	Proper operation of the C/TCE power supply and specifically the +5 Vdc power supply
C038	Temperature, Forward Tube	69 to 73°F	65 to 75°F	Primary or secondary TCS is on and the forward heater is cycling
C039	Temperature, Mirror, C039	69 to 73°F	65 to 75°F	Primary or secondary TCS is on and the forward heater is cycling
C041	Temperature, X-REA 2	68 to 78°F	32 to 104°F	Proper operation of the Beryllium Analog module in the area of the Beryllium proportional counter tube
C141	Temperature, Center Mount Base	69 to 71°F	65 to 75°F	Primary or secondary TCS is on and the center heater is cycling
C143	Temperature, Center Tubes	69 to 72°F	65 to 75°F	Primary or secondary TCS is on and the center heater is cycling
C144	Temperature, Filter/Shutter Mechanisms	69 to 72°F	65 to 75°F	Primary or secondary TCS is on and the aft heater is cycling
C145	Temperature, Camera Interface Plate, (I/P)	69 to 71°F	65 to 75°F	Primary or secondary TCS is on and the aft heater is cycling
M189	Current, I/P High Voltage (HV) Supply Be Counter	58 to 62 mA	45 to 85 mA	X-REA power switch and HV power BE switch are on
M190	Current, I/P High Voltage (HV) Supply AI Counter	58 to 62 mA	45 to 85 mA	X-REA power switch and HV power AL switch are on
M191	Current, I/P Power X-REA	600 to 620 A	550 to .750 A	HV power is on
M192	Current, I/P Power, Camera Electronics	240 to 260 A	200 to 350 A	Camera power switch is on and camera is operating.
M455	Current, Thermal Control	0 to 1.2 A	0 to 1.5 A	Primary or secondary thermal control system is on

TABLE 16. DISCRETE EVENT MEASUREMENTS

MEASUREMENT NUMBER	EVENT	REMARKS
K115	Camera Shutter Open/Closed	A logic 1 indicated shutter open, and logic 0 indicates shutter closed. This measurement will indicate: 1) Camera operating if shutter is cycling. 2) Exposure duration by the time between and open and close indications.
K117	Camera Airlock Open/Closed	A logic 1 indicates airlock open, and logic 0 indicates airlock closed.
K119	Camera Filter Position	A logic 1 indicates filter 1 in position in front of camera. A logic 0 indicates filter 1 not in position. This measurement indicates only filter position 1 and indicates mode selected by time between filter position 1 indications.
K291	Thermal Shield Aperture Door Open	A logic 1 indicates the door is fully open. A logic 0 indicates door in transit, not complete, or closed.
K292	Thermal Shield Aperture Door Closed	A logic 1 indicates the door is fully closed. A logic 0 indicates door in transit, not complete or open.

Figure 11 shows an example of a typical printout of the temperature data on the microfilm. The measurements are given at 1 min intervals. An asterisk following the ground station indicates that the line is "recorded" data; therefore, the values given are not valid.

5056 TEMPERATURE DATA

BATCH 153-3

GMT	C036	C037	C038	C039	C041	C141	C143	C144	C145	STATION
153:14:21	53.459	66.937	69.487	69.658	55.156	69.556	69.663	70.077	69.720	HAU*
153:14:22	53.459	66.937	69.487	69.658	55.156	69.556	69.663	70.077	69.720	HAU*
153:14:23	53.459	66.937	69.487	69.658	55.156	69.556	69.663	70.077	69.720	HAU*
153:14:24	53.459	66.937	69.487	69.658	55.156	69.556	69.663	70.077	69.720	HAU*
153:14:25	53.459	66.937	69.487	69.658	55.156	69.556	69.663	70.077	69.720	HAU*
153:14:26	53.459	66.937	69.487	69.658	55.156	69.556	69.663	70.077	69.720	HAU*
153:14:27	53.459	66.937	69.487	69.658	55.156	69.556	69.663	70.077	69.720	HAU*
153:14:28	53.459	66.937	69.487	69.658	55.156	69.556	69.663	70.077	69.720	HAU*
153:14:29	53.459	66.937	69.487	69.658	55.156	69.556	69.663	70.077	69.720	HAU*
153:14:30	53.459	66.937	69.487	69.658	55.156	69.556	69.663	70.077	69.720	HAU*
153:14:31	53.459	66.937	69.487	69.658	55.156	69.556	69.663	70.077	69.720	HAU*
153:14:32	53.459	66.937	69.487	69.658	55.156	69.556	69.663	70.077	69.720	HAU*
153:14:33	53.459	66.937	69.487	69.658	55.156	69.556	69.663	70.077	69.720	HAU*
153:14:34	53.459	66.937	69.487	69.658	55.156	69.556	69.663	70.077	69.720	HAU*
153:14:35	53.459	66.937	69.487	69.658	55.156	69.556	69.663	70.077	69.720	HAU*
153:14:36	53.459	66.937	69.487	69.658	55.156	69.556	69.663	70.077	69.720	HAU*
153:14:37	53.459	66.937	69.487	69.658	55.156	69.556	69.663	70.077	69.720	HAU*
153:14:38	53.459	66.937	69.487	69.658	55.156	69.556	69.663	70.077	69.720	HAU*
153:14:39	54.323	66.838	69.533	69.963	55.810	69.418	69.479	70.813	69.775	HSK
153:14:40	53.999	67.136	69.671	69.879	55.593	69.501	69.709	70.721	69.830	HSK
153:14:41	53.999	67.136	69.533	69.963	55.593	69.501	69.709	70.721	69.775	HAU*
153:14:42	53.999	67.136	69.533	69.963	55.593	69.501	69.709	70.721	69.775	HAU*
153:14:43	53.999	67.136	69.533	69.963	55.593	69.501	69.709	70.721	69.775	HAU*
153:14:44	53.999	67.136	69.533	69.963	55.593	69.501	69.709	70.721	69.775	HAU*
153:14:45	53.999	67.136	69.533	69.963	55.593	69.501	69.709	70.721	69.775	HAU*
153:14:46	53.999	67.136	69.533	69.963	55.593	69.501	69.709	70.721	69.775	HAU*
153:14:47	53.999	67.136	69.533	69.963	55.593	69.501	69.709	70.721	69.775	HAU*
153:14:48	53.999	67.136	69.533	69.963	55.593	69.501	69.709	70.721	69.775	HAU*
153:14:49	53.999	67.136	69.533	69.963	55.593	69.501	69.709	70.721	69.775	HAU*
153:14:50	53.999	67.136	69.533	69.963	55.593	69.501	69.709	70.721	69.775	HAU*
153:14:51	53.999	67.136	69.533	69.963	55.593	69.501	69.709	70.721	69.775	HAU*
153:14:52	53.999	67.136	69.533	69.963	55.593	69.501	69.709	70.721	69.775	HAU*
153:14:53	53.999	67.136	69.533	69.963	55.593	69.501	69.709	70.721	69.775	HAU*
153:14:54	53.999	67.136	69.533	69.963	55.593	69.501	69.709	70.721	69.775	HAU*
153:14:55	53.999	67.136	69.533	69.963	55.593	69.501	69.709	70.721	69.775	HAU*
153:14:56	53.999	67.136	69.533	69.963	55.593	69.501	69.709	70.721	69.775	HAU*
153:14:57	53.999	67.136	69.533	69.963	55.593	69.501	69.709	70.721	69.775	HAU*
153:14:58	53.999	67.136	69.533	69.963	55.593	69.501	69.709	70.721	69.775	HAU*
153:14:59	54.323	67.335	69.763	70.018	55.702	69.501	69.709	70.353	69.720	HAW
153:15: 0	54.107	67.335	69.579	70.018	55.702	69.556	69.801	70.261	69.830	HAW
153:15: 1	54.323	67.236	69.671	70.073	56.027	69.556	69.709	70.261	69.830	CRO*
153:15: 2	54.323	67.236	69.671	70.073	56.027	69.556	69.709	70.261	69.830	CRO*
153:15: 3	54.323	67.236	69.671	70.073	56.027	69.556	69.709	70.261	69.830	CRO*
153:15: 4	54.323	67.236	69.671	70.073	56.027	69.556	69.709	70.261	69.830	CRO*
153:15: 5	54.323	67.236	69.671	70.073	56.027	69.556	69.709	70.261	69.830	CRO*
153:15: 6	54.323	67.236	69.671	70.073	56.027	69.556	69.709	70.261	69.830	CRO*
153:15: 7	54.323	67.236	69.671	70.073	56.027	69.556	69.709	70.261	69.830	CRO*
153:15: 8	54.323	67.236	69.671	70.073	56.027	69.556	69.709	70.261	69.830	CRO*
153:15: 9	54.323	67.236	69.671	70.073	56.027	69.556	69.709	70.261	69.830	CRO*
153:15:10	54.323	67.236	69.671	70.073	56.027	69.556	69.709	70.261	69.830	CRO*

Note: Temperatures are in degrees Fahrenheit.

Figure 11. Example of printout of S-056 temperature data on microfilm.

Figure 12 shows an example of a typical printout of the discrete event and current data on the microfilm. Again, an asterisk following the ground station indicates that the line is recorded data. The values of the currents on that line are not valid; however, the discrete event values are valid for recorded data as well as for real-time data. A line was printed out in the microfilm record only when one of the discrete event values (K-numbers) changed. Noisy telemetry occasionally caused an inappropriate combination of discrete event values.

The discrete event measurement, K115 (camera shuttle open/close), may be used to determine exposure times for the longer exposures. It has been used in this way to determine exposure times for Super-Long exposures [2]. The operations required to obtain Super-Long exposures created a false set of data in the record because the camera power was turned off. The false line of data is illustrated in Figure 13 which shows the discrete event values associated with a typical Super-Long exposure. The false line contains all zeros except for K291 which indicates that the thermal shield door was open. The use of the times for the various lines to determine the exposure times for the primary and secondary images in the Super-Long frame is also shown in Figure 13.

F. Quantitative Analysis of Filterheliograms

To convert from density on the film to intensity emitted by the Sun, the procedure is as follows.

Density should be converted to exposure (in photons cm^{-2}) at the film by use of Table 13. The table relates exposure to step number in standard sensitometry sets on the film. The density of each step can be measured in any method with any units desired by the user — microdensitometer measurements, microphotometer readings, scanner gray-scale reading, etc. Of course, the density on the solar images must be measured in an identical manner.

The exposure should be divided by the vignetting function at the appropriate distance off-axis. The distance off-axis can be determined with the aid of the information in Section II.D.2; the vignetting function is given in Table 3 and Figure 4. The correction for the vignetting function is often ignored, especially if one is comparing exposures of the same solar feature made close together in time so that the ATM pointing, represented by γX , γY , and γRR , has not changed.

5056 OPERATIONS DATA

BATCH 153-3

GMT	K115	K117	K119	K291	K292	M189	M190	M191	M192	M455	STATION
153:14: 9: 9.006	0	1	0	1	0	-.1605	-.3816	-.0010	.2779	.3785	HAW*
153:14: 9:12.005	1	1	0	1	0	-.1605	-.3816	-.0010	.2779	.3785	HAW*
153:14: 9:20.005	0	1	0	1	0	-.1605	-.3816	-.0010	.2779	.3785	HAW*
153:14: 9:24.005	1	1	0	1	0	-.1605	-.3816	-.0010	.2779	.3785	HAW*
153:14: 9:38.004	0	1	0	1	0	-.1605	-.3816	-.0010	.2779	.3785	HAW*
153:14: 9:42.004	1	1	0	1	0	-.1605	-.3816	-.0010	.2779	.3785	HAW*
153:14: 9:58.003	0	1	0	1	0	-.1605	-.3816	-.0010	.2779	.3785	HAW*
153:14:10: 2.003	1	1	0	1	0	-.1605	-.3816	-.0010	.2779	.3785	HAW*
153:14:10:18.002	0	1	0	1	0	-.1605	-.3816	-.0010	.2779	.3785	HAW*
153:14:10:22.002	0	1	1	1	0	-.1605	-.3816	-.0010	.2779	.3785	HAW*
153:14:10:54.000	1	1	1	0	0	-.1605	-.3816	-.0010	.2779	.3785	HAW*
153:14:11: 6.875	0	1	1	1	0	-.1605	-.3816	-.0010	.2779	.3785	HAW*
153:14:24:37.875	0	1	1	0	0	-.1605	-.3816	-.0010	.2779	.3785	HAW*
153:14:24:49.883	0	1	1	0	1	-.1605	-.3816	-.0010	.2779	.3785	HAW*
153:15: 0:45.126	0	1	1	0	0	59.203	61.120	.6195	.2503	.4123	CRO*
153:15: 0:56.125	0	1	1	1	0	59.203	61.120	.6195	.2503	.4123	CRO*
153:15: 7:56.126	1	1	1	1	0	59.203	61.120	.6195	.2503	.4123	CRO*
153:15: 9:23.129	0	1	1	1	0	59.203	61.120	.6195	.2503	.4123	CRO*
153:15: 9:24.129	0	1	0	1	0	59.203	61.120	.6195	.2503	.4123	CRO*
153:15: 9:26.129	1	1	0	1	0	59.203	61.120	.6195	.2503	.4123	CRO*
153:15: 9:56.128	0	1	0	1	0	59.203	61.120	.6195	.2503	.4123	CRO*
153:15: 9:59.127	1	1	0	1	0	59.203	61.120	.6195	.2503	.4123	CRO*
153:15:10:48.125	0	1	0	1	0	59.203	61.120	.6195	.2503	.4123	CRO*
153:15:10:52.125	1	1	0	1	0	59.203	61.120	.6195	.2503	.4123	CRO*
153:15:11:48.130	0	1	0	1	0	59.203	61.120	.6195	.2503	.4123	CRO*
153:15:11:50.880	1	1	0	1	0	59.203	61.120	.6195	.2492	.4092	GDS
153:15:12:44.127	0	1	0	1	0	60.039	61.434	.6154	.2523	.4092	CRO*
153:15:12:49.127	0	1	1	1	0	60.039	61.434	.6154	.2523	.4092	CRO*
153:15:20:30.125	1	1	1	1	0	60.039	61.434	.6154	.2523	.4092	CRO*
153:15:20:34.125	0	1	1	1	0	60.039	61.434	.6154	.2523	.4092	CRO*
153:15:20:35.125	0	1	0	1	0	60.039	61.434	.6154	.2523	.4092	CRO*
153:15:20:38.125	1	1	0	1	0	60.039	61.434	.6154	.2523	.4092	CRO*
153:15:20:42.882	0	1	0	1	0	60.039	61.434	.6154	.2523	.4092	CRO*
153:15:20:46.882	1	1	0	1	0	60.039	61.434	.6154	.2523	.4092	CRO*
153:15:20:50.882	0	1	0	1	0	60.039	61.434	.6195	.2564	.4092	MIL
153:15:20:51.382	0	1	1	1	0	60.666	60.596	.6144	.2523	.4092	MIL
153:15:20:54.132	1	1	1	1	0	59.725	61.120	.6113	.2492	.4092	MIL
153:15:20:58.881	0	1	0	1	0	60.039	60.806	.6195	.2564	.4092	MIL
153:15:21: 2.381	1	1	0	1	0	60.039	60.806	.6133	.2523	.4092	MIL
153:15:21: 6.881	0	1	0	1	0	60.039	60.596	.6164	.2492	.4092	MIL
153:15:21:10.881	1	1	0	1	0	60.561	60.387	.6154	.2523	.4092	MIL
153:15:21:14.881	0	1	0	1	0	60.248	61.120	.6174	.2523	.4062	MIL
153:15:21:16.131	0	1	1	1	0	60.039	60.177	.6144	.2554	.4092	MIL
153:15:21:19.130	1	1	1	1	0	60.039	61.434	.6133	.2523	.4092	MIL
153:15:21:23.630	0	1	0	1	0	60.039	60.282	.6174	.2615	.4123	MIL
153:15:21:27.130	1	1	0	1	0	59.830	60.177	.6092	.2523	.4092	MIL
153:15:21:31.630	0	1	0	1	0	60.039	60.177	.6144	.2503	.4046	MIL
153:15:21:35.629	1	1	0	1	0	60.248	60.282	.6113	.2523	.4092	MIL
153:15:21:39.879	0	1	0	1	0	60.457	60.282	.6133	.2779	.4062	MIL
153:15:21:40.879	0	1	1	1	0	60.039	61.015	.6195	.2492	.0462	MIL

Note: Currents M189 and M190 are in milliamperes. Currents M191, M192, and M455 are in amperes.

Figure 12. Example of printout of S-056 discrete event and current data on microfilm.

REPRODUCIBILITY OF THE
ORIGINAL PAGE IS POOR

GMT	K115	K117	K119	K291	K292	
363:14:18:24.250	1	1	1	1	0	Primary Exposure \approx 5m 48 s
363:14:18:26.250	0	0	0	1	0	
363:14:24:12.250	1	1	1	1	0	Secondary Exposure \approx 9 s
363:14:24:21.250	0	1	1	1	0	

Figure 13. Example of discrete event data associated with a Super-Long exposure (Filter 1).

If desired, the exposure distribution of a portion of an image can then be deconvolved using the point spread function given in Table 2 and Figure 3 and discussed in Section II.A.2. Such operations are usually performed with Fourier transform techniques.

The result of the preceding steps is a value (or distribution of values over an image) of the corrected exposure, Φ_n (in photons cm^{-2}), at the film, where n denotes the filter. The corrected exposure should then be divided by the exposure time, t, to yield the corrected photon flux, Φ_n/t (in photons $\text{cm}^{-2} \text{s}^{-1}$), at the film. The exposure time can be obtained from the data block lights for the particular frame (Section II.D.3) or the microfilm records (Section II.E), or the values given in Table 6 can be used.

The photon flux should be multiplied by the square of the focal length, f, and divided by the telescope collecting area, A_T , to obtain the photon intensity integrated over the filter bandpass (in photons $\text{cm}^{-2} \text{s}^{-1} \text{sr}^{-1}$); i.e.,

$$\int \eta_n(\lambda) \frac{I_\lambda(\lambda)}{h\nu} d\lambda = \frac{f^2}{A_T t} \Phi_n ,$$

where η_n is the combined filter-telescope transmission for filter n for photons at wavelength λ (given in Table 5 and Figs. 5 through 7), $h\nu$ is the energy per photon, and I_λ is the usual specific intensity (or radiance) used in astrophysics (in $\text{erg cm}^{-2} \text{s}^{-1} \text{sr}^{-1} \text{\AA}^{-1}$). The focal length and telescope aperture area are given in Table 1.

Further interpretation of the data in terms of emission coefficients, temperatures, emission measures, and densities on the Sun requires the introduction of assumed spectra. One usually computes theoretical spectra for optically thin thermal plasmas of coronal temperatures and composition. The computed spectra are then multiplied by $\eta(\lambda)$, the filter transmission multiplied by the mirror reflectivities, and integrated over the wavelength band. The results of the computations for the different filters can then be compared with the observations.

Although the previously mentioned procedure is straightforward, there are pitfalls of which to be wary. First is the use of copies instead of the original flight film. It is extremely difficult to avoid nonuniformity in the copying process. Resolution of small-scale features will also be degraded. Another possible problem is the use of wavelength-invariant characteristic curves (where exposure is given in photons rather than energy), especially at the long wavelengths passed by Filter 3. Other errors can arise from the usual problems associated with photographic photometry — e.g., inaccuracies in determining the characteristic curve and errors in measuring density, especially of small features on the film.

III. X-RAY EVENT ANALYZER

A. Instrument Description

The X-REA consisted of two proportional counters and associated electronics which monitored the soft X-ray flux from the entire Sun and provided a time history of the variation of emission from flares and other transient events. The position of the X-REA in the S-056 package is shown in Figure 1. The X-REA operated continuously whenever the X-ray telescope was being used. In addition, the X-REA could be operated during unattended periods when the thermal shield door was open, as was the case during SL3. The X-REA is described in more detail in Reference 3 and in "The Skylab ATM/S-056 Solar X-Ray Telescope: Design and Performance," to be published in 1977.

The two detectors were conventional coaxial counters, gas-filled to 1 atm. The "soft" detector (usually called the aluminum counter) had an aluminum window supported by an 80 percent transmitting aluminum mesh and counted X-rays between the nominal wavelengths of 6.1 and 20 Å. The "hard" detector (usually called the beryllium counter) had a beryllium window and

counted X-rays between the nominal wavelengths of 2.5 and 7.25 Å. Pulse-height analysis was used to separate the signals into various wavelength channels and thus provide coarse spectra. There were four channels for the aluminum counter and six channels for the beryllium counter. Both counters had integration times of 2.5 s, and all channels were read out every 2.5 s.

A four-position aperture wheel in front of each counter window increased the dynamic range of the X-REA. Each aperture was a factor of approximately four different in area from the next window. The apertures could be changed manually by the astronaut at the control panel or automatically (as usually used) when the counting rate reached a certain level.

The important X-REA properties are summarized in Table 17. Some of the temperature and current measurements listed in Table 15 and available on microfilm (with examples shown in Figs. 11 and 12) are relevant to the X-REA. However, all of the temperatures and currents stayed within the normal operating range throughout the mission.

TABLE 17. X-RAY EVENT ANALYZER PROPERTIES

		ALUMINUM COUNTER		BERYLLIUM COUNTER
Window Material and Thickness		0.25 mil (6.35 µm) Aluminum		10 mil (254 µm) Beryllium
Window Thickness (mg cm ⁻²)		1.71		47
Gas Mixture		90% Argon 10% Methane		90% Xenon 10% Methane
Aperture Area (cm ²)	Aperture	1 2 3 4	2.45 (-3) 5.35 (-3) 2.04 (-2) 7.92 (-2)	2.04 (-2) 8.11 (-2) 3.22 (-1) 1.27 (0)
Nominal Channel Boundary Wavelengths at Start of Mission (Å)	Channel	1 2 3 4 5 6	16.0 to 20.0 12.0 to 16.0 8.0 to 12.0 6.1 to 8.0	6.00 to 7.25 5.50 to 6.00 5.00 to 5.50 4.50 to 5.00 3.75 to 4.50 2.50 to 3.75

B. Proportional Counter Response

The response of the various channels of the two proportional counters at the beginning of the Skylab mission to photons of different wavelengths is given in Tables 18 and 19 and is shown in Figures 14 and 15. The response is the probability of a count appearing in a channel for each photon as a function of wavelength of the photon. The response of each channel extends beyond the wavelength boundaries given in Table 17 because of the finite energy-resolution width inherent in proportional counters.

Also presented in the figures is the "total" counter efficiency, the product of the window transmission and the absorption efficiency of the gas. (The "total" response is greater than the sum of the responses of the individual channels because the pulse-height analyzers excluded photons whose apparent energies were outside the extreme limits of the highest and lowest channels.) As can be seen, the strong wavelength dependence of the efficiency sometimes dominates the variation of the response so that the peak of the response function for a particular channel can occur outside its nominal wavelength boundaries.

At the start of the mission, the counters exhibited excessively large count rates in the low-energy, long-wavelength channels. The cause of the low-energy excess is not yet understood, and those channels should be avoided or used with caution.

The performance of the counters degraded during the mission. The gain changed so that the wavelength boundaries of the channels and the counter efficiency also changed. Caution is advised in the use of the absolute values of the count rates and the channel ratios for all channels after the first manned mission (SL2).

C. X-REA Observations

1. Microfilm Records. The scientific data from the X-REA are included in the 565 rolls of microfilm records submitted to the NSSDC which also contain the current, temperature, and discrete event measurements described earlier. The 6 h periods corresponding to the individual records are presented in Table 14. Figure 16 shows the format of the records. The basic data consist of the counts accumulated for 2.5 s for each channel as a function of time (at 2.5 s intervals). Also presented are the sums of the counts in all channels for each counter and the aperture positions. An asterisk following the ground station abbreviation indicates that the data came from the recorder. (The X-REA data

TABLE 18. ALUMINUM COUNTER RESPONSE

WAVELENGTH (Å)	CHANNEL			
	1	2	3	4
4.5				9.30(-4)
5.0				4.50(-3)
5.5			2.60(-4)	9.35(-3)
6.0			6.61(-4)	1.06(-2)
6.5			9.91(-4)	7.41(-3)
7.0			9.60(-4)	3.51(-3)
7.5			6.45(-4)	1.21(-3)
7.95-			3.45(-4)	3.62(-4)
7.95+	1.50(-4)	5.03(-3)	2.10(-1)	2.20(-1)
8.0	1.67(-4)	5.45(-3)	2.15(-1)	2.12(-1)
8.5	4.31(-4)	1.12(-2)	2.54(-1)	1.35(-1)
9.0	9.48(-4)	1.97(-2)	2.65(-1)	7.68(-2)
9.5	1.82(-3)	3.02(-2)	2.51(-1)	3.95(-2)
10.0	3.10(-3)	4.13(-2)	2.19(-1)	1.86(-2)
10.5	4.76(-3)	5.12(-2)	1.80(-1)	8.08(-3)
11.0	6.68(-3)	5.83(-2)	1.40(-1)	3.27(-3)
11.5	8.66(-3)	6.15(-2)	1.03(-1)	1.24(-3)
12.0	1.04(-2)	6.06(-2)	7.28(-2)	4.41(-4)
12.5	1.18(-2)	5.61(-2)	4.93(-2)	1.49(-4)
13.0	1.25(-2)	4.93(-2)	3.21(-2)	
13.5	1.26(-2)	4.11(-2)	2.01(-2)	
14.0	1.21(-2)	3.27(-2)	1.21(-2)	
14.5	1.11(-2)	2.50(-2)	7.04(-3)	
15.0	9.66(-3)	1.83(-2)	3.96(-3)	
15.5	8.10(-3)	1.29(-2)	2.15(-3)	
16.0	6.52(-3)	8.82(-3)	1.13(-3)	
16.5	5.06(-3)	5.81(-3)	5.75(-4)	
17.0	3.78(-3)	3.70(-3)	2.83(-4)	
17.5	2.73(-3)	2.29(-3)	1.35(-4)	
18.0	1.91(-3)	1.37(-3)		
18.5	1.29(-3)	7.98(-4)		
19.0	8.45(-4)	4.51(-4)		
19.5	5.37(-4)	2.48(-4)		
20.0	3.31(-4)	1.33(-4)		
20.5	1.98(-4)			
21.0	1.15(-4)			

Note: Measurements given in (counts photon⁻¹).

TABLE 19. BERYLLIUM COUNTER RESPONSE

WAVELENGTH (Å)	CHANNEL					
	1	2	3	4	5	6
1.8						4.61(-4)
2.0						9.94(-3)
2.2						7.73(-2)
2.4						2.70(-1)
2.6					4.74(-4)	4.93(-1)
2.8					3.33(-3)	6.53(-1)
3.0				2.53(-4)	1.49(-2)	6.68(-1)
3.2			1.08(-4)	1.25(-3)	4.56(-2)	5.98(-1)
3.4			4.92(-4)	4.60(-3)	1.02(-1)	4.84(-1)
3.6		2.23(-4)	1.73(-3)	1.29(-2)	1.72(-1)	3.47(-1)
3.8	1.34(-4)	7.37(-4)	4.85(-3)	2.84(-2)	2.29(-1)	2.14(-1)
4.0	4.22(-4)	2.00(-3)	1.10(-2)	5.03(-2)	2.46(-1)	1.12(-1)
4.2	1.12(-3)	4.55(-3)	2.08(-2)	7.33(-2)	2.19(-1)	4.96(-2)
4.4	2.53(-3)	8.75(-3)	3.29(-2)	8.90(-2)	1.66(-1)	1.84(-2)
4.6	4.99(-3)	1.45(-2)	4.45(-2)	9.15(-2)	1.08(-1)	5.72(-3)
4.8	8.60(-3)	2.07(-2)	5.19(-2)	8.07(-2)	6.15(-2)	1.50(-3)
5.0	1.31(-2)	2.61(-2)	5.28(-2)	6.17(-2)	3.07(-2)	3.36(-4)
5.2	1.79(-2)	2.90(-2)	4.72(-2)	4.12(-2)	1.36(-2)	
5.4	2.20(-2)	2.87(-2)	3.74(-2)	2.43(-2)	5.32(-3)	
5.6	2.45(-2)	2.55(-2)	2.64(-2)	1.28(-2)	1.86(-3)	
5.8	2.48(-2)	2.04(-2)	1.67(-2)	5.98(-3)	5.79(-4)	
6.0	2.30(-2)	1.47(-2)	9.56(-3)	2.57(-3)	1.62(-4)	
6.2	1.96(-2)	9.69(-3)	4.96(-3)	9.57(-4)		
6.4	1.55(-2)	5.82(-3)	2.34(-3)	3.30(-4)		
6.6	1.14(-2)	3.20(-3)	1.01(-3)	1.03(-4)		
6.8	7.76(-3)	1.62(-3)	3.97(-4)			
7.0	4.95(-3)	7.53(-4)	1.44(-4)			
7.2	2.95(-3)	3.24(-4)				
7.4	1.65(-3)	1.29(-4)				
7.6	8.71(-4)					
7.8	4.31(-4)					
8.0	2.01(-4)					

Note: Measurements given in (counts photon⁻¹).

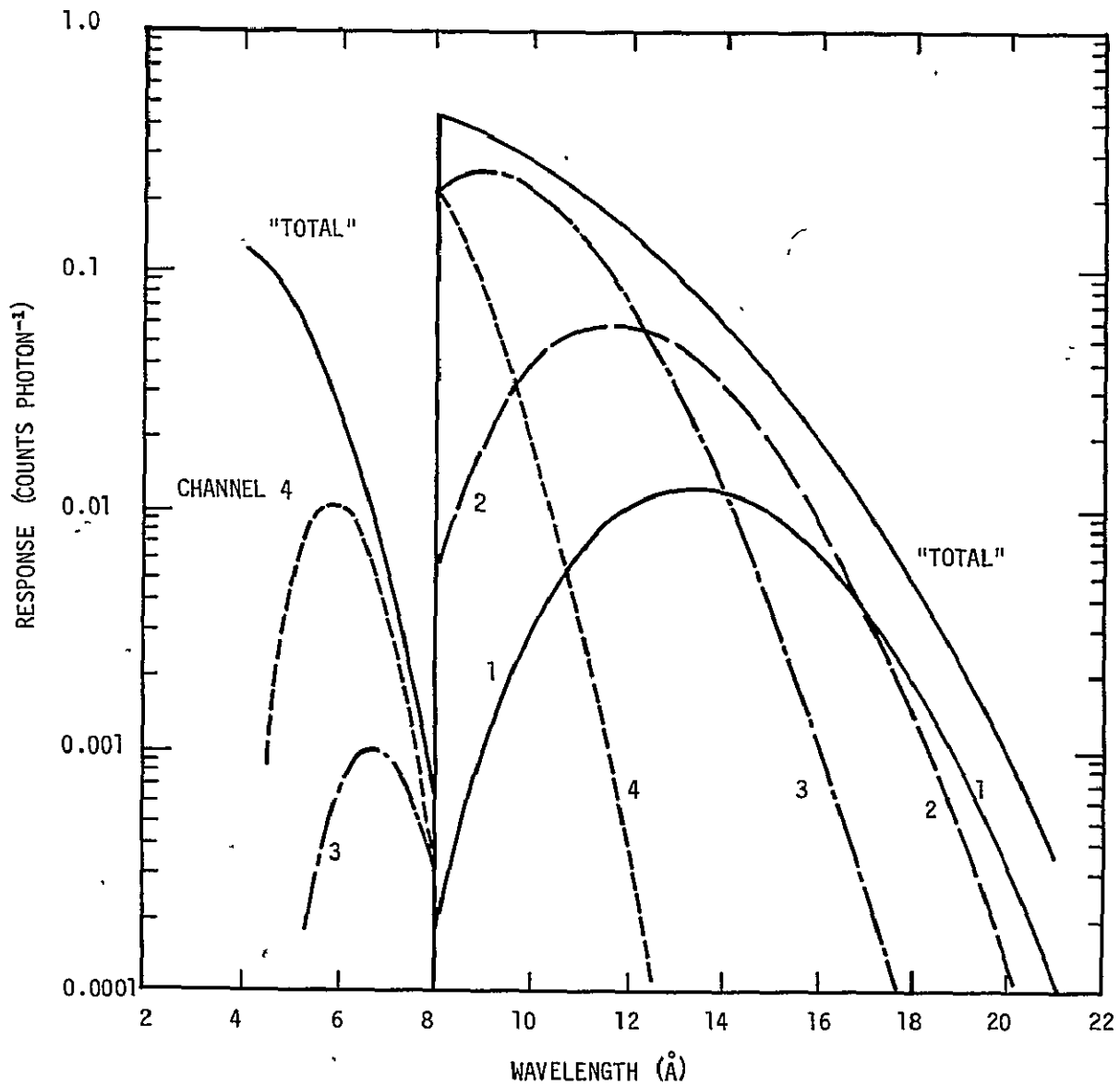


Figure 14. Aluminum counter response.

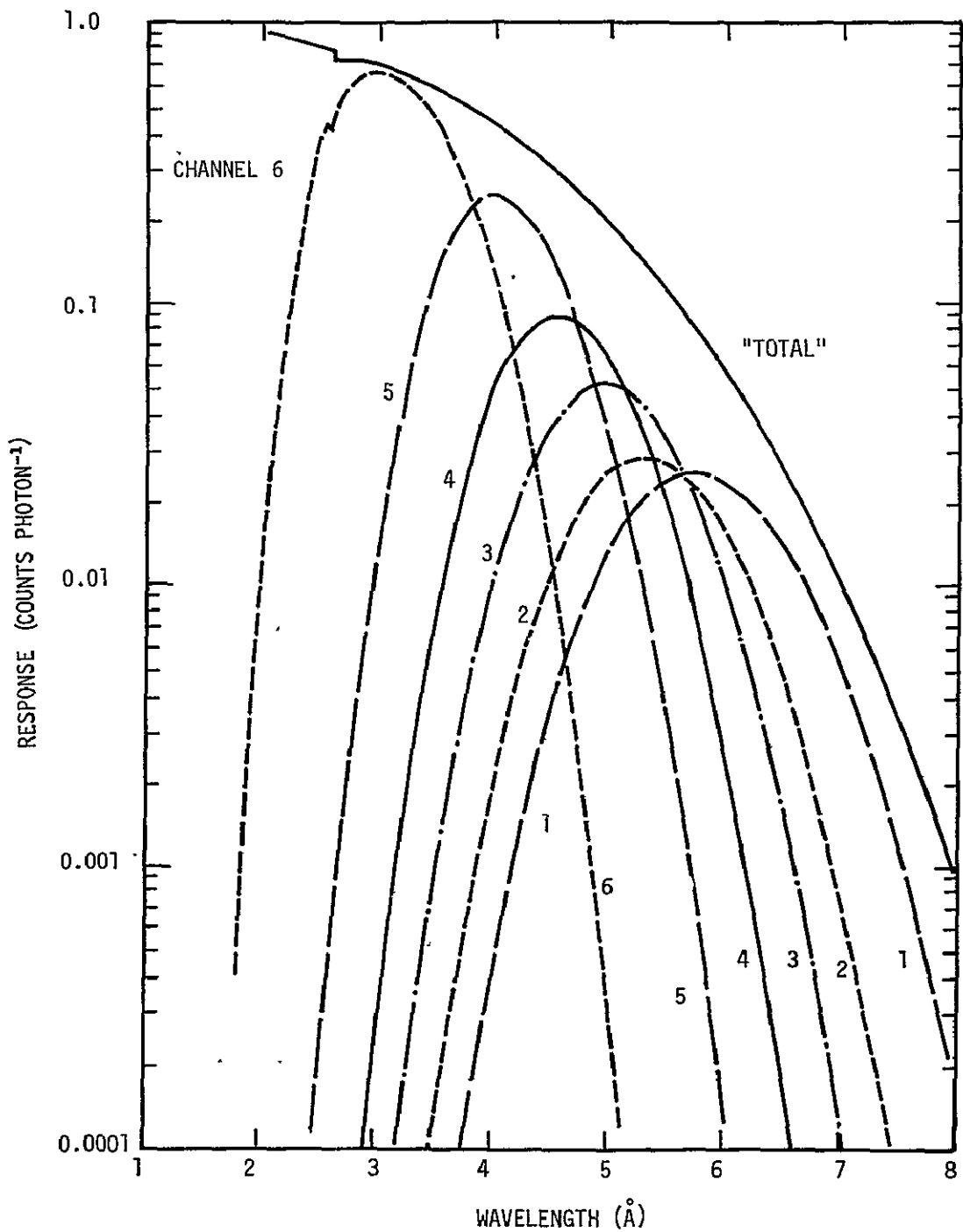


Figure 15. Beryllium counter response.

GMT		APER		XREA SCIENTIFIC DATA K0113-056						BATCH 153-3						APER		STATION	
		POS		ALUMINUM			TOTALS			BERILLIUM					POS				
				1	2	3	4	AL	BE	1	2	3	4	5	6				
153	14 53 39 6	1		0	7	0	0	7	23315	401	0	0	12080	10834	0	4	HAW*		
153	14 53 42 1	1		0	7	0	0	7	23315	401	0	0	12080	10834	0	4	HAW*		
153	14 53 44 6	1		0	7	0	0	7	23315	401	0	0	12080	10834	0	4	HAW*		
153	14 53 47 1	1		0	7	0	0	7	23315	401	0	0	12080	10834	0	4	HAW*		
153	14 53 49 6	1		0	7	0	0	7	23315	401	0	0	12080	10834	0	4	HAW*		
153	14 53 52 1	1		0	7	0	0	7	23315	401	0	0	12080	10834	0	4	HAW*		
153	14 59 54 6	1	2212	2221	2217	2216	8866	8950	1492	1481	1416	1565	1502	1494	1	HAW			
153	14 59-57 1	1	2211	2222	2216	2216	8865	8952	1492	1483	1431	1546	1505	1495	1	HAW			
153	14 59 59 6	1	2387	2180	2025	2217	8809	8952	1492	1482	1436	1547	1502	1493	1	HAW			
153	15 0 27 1	4	0	0	0	1	1	10		1	2	1	1	1	4	4	HAW		
153	15 0 29 6	4	0	0	3	2	5	11		4	1	0	1	1	4	4	HAW		
153	15 0 32 1	4	4	1	1	1	7	13		1	1	2	0	2	7	4	HAW		
153	15 0 34 6	4	0	0	1	0	1	11		3	0	0	2	3	3	4	HAW		
153	15 0 37 1	4	2	1	1	3	7	9		2	0	0	1	0	6	4	CRO*		
153	15 0 39 6	4	0	1	2	1	4	6		1	1	0	0	0	4	4	CRO*		
153	15 0 42 1	4	1	0	2	1	4	9		2	0	0	2	0	5	4	CRO*		
153	15 0 44 6	4	0	0	2	2	4	6		3	0	0	0	0	3	4	CRO*		
153	15 1 29 6	4	70	451	557	50	1128	264	113	47	38	33	21	12	4	CRO*			
153	15 1 27 1	4	233	1140	1312	81	2816	445	201	80	85	46	24	9	4	CRO*			
153	15 1 29 6	3	476	1375	1926	54	3831	513	242	93	70	62	33	13	4	CPO*			
153	15 1 32 1	3	216	669	1606	36	2527	554	282	100	86	49	30	7	4	CRO*			
153	15 1 34 6	3	342	934	797	25	2098	594	318	90	95	50	35	6	4	CRO*			
153	15 1 37 1	3	510	1121	995	30	2556	658	351	116	78	66	32	15	4	CRO*			
153	15 1 39 6	3	686	1431	1013	22	3152	648	347	107	94	64	33	3	4	CRO*			
153	15 1 42 1	3	827	1510	1090	27	3454	611	371	120	87	49	32	12	4	CRO*			
153	15 1 44 6	3	1000	1758	1167	20	3945	690	391	101	82	68	39	7	4	CRO*			
153	15 1 47 1	3	1073	1800	1247	21	4141	684	374	119	90	54	39	8	4	CRO*			
153	15 1 49 6	3	1111	1965	1223	33	4332	679	365	113	85	60	43	13	4	CRO*			
153	15 1 52 1	3	1274	1994	1266	25	4559	687	371	114	95	58	39	10	4	CRO*			
153	15 1 54 6	3	1306	2041	1284	21	4652	689	369	123	92	64	31	10	4	CRO*			
153	15 1 57 1	3	1380	2204	1316	25	4927	690	374	123	101	47	31	14	4	CRO*			
153	15 1 59 6	3	1384	2142	1336	28	4890	721	403	125	85	60	35	13	4	CRO*			
153	15 2 2 1	3	1352	2184	1357	27	4920	689	379	116	97	51	37	9	4	CRO*			
153	15 2 4 6	3	1455	2214	1353	32	5054	698	376	133	87	58	33	11	4	CRO*			
153	15 2 7 1	2	972	1382	1391	20	3165	715	400	107	100	65	34	9	4	CRO*			
153	15 2 9 6	2	466	767	784	13	2030	690	389	125	81	60	27	8	4	CRO*			
153	15 2 12 1	2	491	790	517	13	1011	738	401	139	101	58	35	4	4	CPO*			
153	15 2 14 6	2	433	804	526	13	1776	703	416	108	85	59	31	4	4	CRO*			

Note: The four sets of data illustrate (a) counters off, (b) calibration mode, (c) background counts with counters on and thermal shield door closed, and (d) solar observations with counters on and door open. The solar observations also illustrate aperture changes caused by an increasing count rate during a sunrise.

Figure 16. Example of printouts of S-056 X-REA data on microfilm.

were both telemetered in real time when Skylab was in range of a ground station and recorded on board for later transmission; however, this information is normally not important to users.)

The X-REA data are also available at the experimenters' institutions on magnetic tape and on printouts.

Essentially, the data recorded in the microfilm records are "raw" in that no background counts have been removed, nor has any correction factor been applied to the data to adjust it for degradation of the counters with time. X-REA data immediately following an aperture position change should be discarded because the aperture wheel may have changed during the 2.5 s accumulation. Sometimes, two lines of readout must be discarded, apparently due to noise spikes associated with the aperture change. Also, on occasion, the telemetry record indicates an incorrect aperture position for the counters which is apparent only when data from both counters prior to, during, and following the period of interest are compared. The spurious aperture indication has been particularly noted in data from the SL3 mission.

Typical X-REA data fall into four categories, as shown in Figure 16. First, when the counters are off, the readings are asterisks, zeros, or constant numbers (generally in only one or two channels). Second, when the X-REA was placed in the "calibration mode," a predetermined number appeared in all channels and total counts columns. The calibration signal verified the operation of the counter electronics only. No calibration source to verify the counter gas response was employed in the instrument. Third, when the counters were on with the thermal shield door closed, the readings indicate background counts. These counts increased during passages through the South Atlantic Anomaly (SAA) and the "horns" of the Van Allen radiation belts. Finally, when the counters were on and the door was open, the readings reflect the counts due to X-rays from the Sun. Again, these solar counting rates were occasionally contaminated with high background counts due to the SAA and the "horns."

2. Specialized Catalog. The X-REA observing periods have been correlated with solar flare activity during the Skylab mission. The results will be given in a forthcoming report, "Skylab ATM/S-056 X-Ray Event Analyzer Observations Versus Solar Flare Activity: An Event Compilation," which will list all flares that occurred during each period when the X-REA was operating.

D. Quantitative Analysis of X-REA Observations

The interpretation of the counts described in Section III. C in terms of the X-ray flux emitted by the Sun involves the following procedure.

The observed counts, Ψ_n , as given on the microfilm, where n denotes the channel, were accumulated for a time, t (equal to 2.5 s), and with an aperture also indicated on the microfilm. Therefore, Ψ_n should be divided by t and then divided by the aperture area, A , to obtain the solar photon flux at the detector integrated over the response of the channel; i. e.,

$$\int \eta_n(\lambda) \phi_\lambda(\lambda) d\lambda = \frac{\Psi_n}{At} \quad (\text{in photons cm}^{-2} \text{ s}^{-1}) ,$$

where $\eta_n(\lambda)$ is the probability of a count appearing in channel n per photon at wavelength λ (analogous to the filter-telescope transmission used in Section II. F for the X-ray telescope) and ϕ_λ is the solar photon flux incident on the detector (in photons $\text{cm}^{-2} \text{ s}^{-1} \text{ \AA}^{-1}$). The aperture area is given in Table 17, and η_n is given in Tables 18 and 19 and Figures 14 and 15. The solar flux is related to the intensity, I_λ , mentioned in Section II. F, by

$$\phi_\lambda = \int \frac{I_\lambda}{h\nu} d\Omega ,$$

where $h\nu$ is the energy per photon and the integral over solid angle Ω covers the field-of-view (in this case, the entire Sun as seen from the observing instrument).

As before, the further interpretation of the data requires the introduction of assumed spectra. The spectra, usually theoretical spectra for an optically thin plasma of coronal composition and temperature, are multiplied by η_n and integrated over the wavelength band. The results are then compared with the observations. Wilson [3] has given an example of such an analysis.

In general, extreme caution is advised in the quantitative interpretation of the X-REA observations. Prospective users are urged to contact the S-056 data analysis groups before doing any quantitative work.

REFERENCES

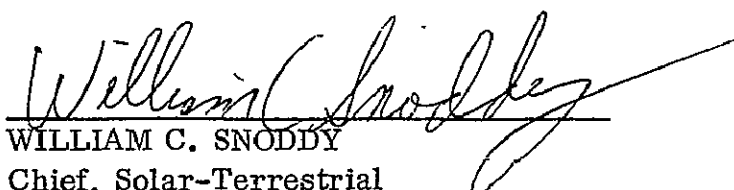
1. White, A. F.: MSFC Skylab Apollo Telescope Mount Experiment Systems Mission Evaluation. NASA TM X-64821, Marshall Space Flight Center, Alabama, 1974.
2. Wilson, R. M.: Atlas of Skylab ATM/S056 Super-Long Exposures and Stepped-Image Frames. NASA TM X-64992, Marshall Space Flight Center, Alabama, 1976.
3. Wilson, R. M.: The Skylab ATM/S-056 X-Ray Event Analyzer: Instrument Description, Parameter Determination, and Analysis Example (15 June 1973 1B/M3 Flare). NASA TM X-78332, Marshall Space Flight Center, Alabama, 1976.
4. Speich, D. M.; Smith, J. B.; Reichmann, E. J.; McGuire, J. P.; Underwood, J. H.; Vorpahl, J. A.; and McKenzie, D. L.: Compilation of Flares and Transients Observed by the S-056 Solar X-Ray Telescope During the Skylab Missions. NASA TM X-73346, Marshall Space Flight Center, Alabama, 1976.
5. Wilson, R. M.: Atlas of Skylab ATM/S056 Coronal Hole Observations. NASA TM X-64994, Marshall Space Flight Center, Alabama, 1976.
6. Walsh, E. J.; Sokolowski, T. I.; Miller, G. M.; Cofield, K. L.; Douglas, J. D.; Lewter, B. J.; Burke, H. O.; and Davis, A. J.: Design Characteristics of a Skylab Soft X-Ray Telescope. Proc. Soc. Photo-Optical Instr. Engineers, vol. 44, 1974, pp. 175-184.
7. Underwood, J. H.; Milligan, J. E.; deLoach, A. C.; and Hoover, R. B.: The S-056 X-Ray Telescope Experiment on the Skylab-Apollo Telescope Mount. Applied Optics, vol. 16, 1977 (in press).
8. Pem, J. P.: ATM Mission Operation Log. Vols. 1-5, Ball Brothers Research Corporation, Boulder, Colorado, 1975.
9. Fowler, W. K.: Skylab Apollo Telescope Mount Pointing Reference Handbook. Ball Brothers Research Corporation TN 74-27, 1974.
10. Fowler, W. K.: Roll Reference Determination Summary Report. Ball Brothers Research Corporation, TN 75-14, 1975.

APPROVAL

USERS' GUIDE TO THE DATA OBTAINED BY THE SKYLAB/ATM NASA-MARSHALL SPACE FLIGHT CENTER/THE AEROSPACE CORPORATION S-056 X-RAY EXPERIMENT

The information in this report has been reviewed for security classification. Review of any information concerning Department of Defense or Atomic Energy Commission programs has been made by the MSFC Security Classification Officer. This report, in its entirety, has been determined to be unclassified.

This document has also been reviewed and approved for technical accuracy.



WILLIAM C. SNODDY
Chief, Solar-Terrestrial
Physics Division



CHARLES A. LUNDQUIST
Director, Space Sciences Laboratory